DOCTORAL (Ph.D.) DISSERTATION

Optimization of manufacture and examination of micropellets based on pharmaceutical technological and biopharmaceutical parameters

Dr. Szilárd Pál

University of Pécs, Faculty of Medicine

Institute of Pharmaceutical Technology and Biopharmacy

Pécs

2013

Optimization of manufacture and examination of micropellets based on pharmaceutical technological and biopharmaceutical parameters

Dr. Szilárd Pál

Head of the Doctoral School:

Dr. Erika Pintér

Head of Program:

Dr. Loránd Barthó

Supervisor:

Dr. Attila Dévay

Founder and first director of

the Institute of Pharmaceutical Technology and Biopharmacy

University of Pécs, Faculty of Medicine

Pécs

2013

Publications and presentations related to the thesis

1. **Sz. Pál**, S. Nagy, T. Bozó, B. Kocsis, A. Dévay:
   Technological and biopharmaceutical optimization of nystatin release from a multiparticulate based bioadhesive drug delivery system
   European Journal of Pharmaceutical Sciences 49.2: 258-264.2013.
   IF: 3.212

2. S. Nagy, B. Kocsis, **Sz. Pál**, T. Bozó, K. Mayer, A. Dévay:
   Antifungális hatóanyagtartalmú bioadhezív mikropelletek vizsgálati tapasztalatai
   XVI. Gyógyszertechnológiai Konferencia és VIII. Gyógyszer az ezredfordulón Konferencia, Siófok, 2010.

3. A. Dévay, B. Kocsis, **Sz. Pál**, K. Mayer, S. Nagy:
   Quick detection of *Nystatin* from sustained release dosage forms using Microbiologically Detected Dissolution (MDD)
   The 2nd BBBB Conference on Pharmaceutical Sciences, Tartu, 2007.

4. **Sz. Pál**, K. Mayer, I. Antal, A. Dévay:
   Comparison of evaluation on pharmaceutical and biopharmaceutical properties of multiparticular dosage forms using factorial design and artificial neural network
   The 2nd BBBB Conference on Pharmaceutical Sciences, Tartu, 2007.

5. A. Dévay, K. Mayer, **Sz. Pál**, I. Antal:
   Investigation on drug dissolution and particle characteristics of pellets related to manufacturing process variables of high-shear granulation
   Journal of Biochemical and Biophysical Methods 69: 197-205.2006.
   IF: 1.302

6. A. Dévay, S. Nagy, **Sz. Pál**:
   MDD, új eljárás antibiotikumok kioldódásának vizsgálatára
   Congressus Pharmaceuticus Hungaricus XIII., Budapest, 2006.

7. A. Dévay, S. Nagy, **Sz. Pál**:
   Comparison of dissolution and microbiological thin layer chromatography detection of drugs containing antimicrobial drugs
   5th World Meeting on Pharmaceutics, Biopharmaceutics and Pharmaceutical Technology, Geneva, 2006.

8. A. Dévay, **Sz. Pál**, S. Nagy:
   A mikrobiológiailag detektált kioldódási (MDD) módszer alkalmazása antifungális hatóanyagtartalom érzékeny és gyors vizsgálatára
   Gyógyszerkutatási Szimpózium, Debrecen, 2006.

9. A. Dévay, I. Antal, **Sz. Pál**:
   Gyógyszeres mikropelletek formulálásásának szempontjai
   Gyógyszerkutatási Szimpózium, Debrecen, 2006.

10. A. Dévay, K. Mayer, **Sz. Pál**:
    Investigation of dissolution of active ingredient from micropellets
    8th Symposium on Instrumental Analysis, Graz, 2005.

11. A. Dévay, B. Kocsis, **Sz. Pál**, A. Bodor, K. Mayer, S. Nagy:
    Application of a microbiological detection for investigation of dissolution of antibiotic delivery systems
    8th Symposium on Instrumental Analysis, Graz, 2005.

12. A. Dévay, **Sz. Pál**, I. Antal:
    Effect of process parameters on characteristics of *theophylline* containing pellets prepared in high shear granulator
    6th Central European Symposium on pharmaceutical technology and biotechnology, Siófok, 2005.

Other publications

1. Gy. Horváth, É. Szőke, Á. Kemény, T. Bagoly, J. Deli, L. Szente, **Sz. Pál**, K. Sándor, J. Szolcsányi, Zs. Helyes:
   Lutein inhibits the function of the transient receptor potential A1 ion channel in different in vitro and in vivo models.
   Journal of Molecular Neuroscience 1: 1-9.2012.
   IF: 2.922

2. **Sz. Pál**, A. Dévay:
   A kronoterápia gyógyszerészeti vonatkozásai
   Gyógyszerészet 55:131-137.2011.

3. A. Dévay, **Sz. Pál:**
   Kronoterápiás hatóanyagleadó rendszerek tervezése
   Gyógyszerészet 55:323-328.2011.

4. S. Merczel, **Sz. Pál**, B. Kocsis, A. Dévay:
   PVP-J tartalmú biokompatibilis műkönnyek gyógyszertechnológiai és mikrobiológiai optimalizálása
   Acta Pharmaceutica Hungarica 80:59-66.2010.

5. T. Bozó, K. Mayer, **Sz. Pál**, A. Dévay:
   A szem korszerű gyógyszeres terápiájának lehetőségei
   Gyógyszerészet 53:5-12.2009.

6. T. Bozó, **Sz. Pál**, A. Dévay:
   Liposzómák fejlesztésének és gyógyszerterápiás alkalmazásának újabb lehetőségei
   Acta Pharmaceutica Hungarica 78:103-109. 2008.

7. **Sz. Pál**, K. Mayer, A. Dévay:
   Részecskeméret-meghatározás a dinamikus fényszóródás módszerével
   Acta Pharmaceutica Hungarica 75:23-31.2005.

8. **Sz. Pál:**
   A patikus dilemmái: a FoNo VII. a gyakorlatban
   Acta Pharmaceutica Hungarica 75:199-203.2005.

Other presentations

1. A. Dévay, **Sz. Pál**:
   Preparation and examination of cochleates using central composite design
   6th Central European Symposyum on pharmaceutical technology and biotechnology, Siófok, 2005.

2. A. Dévay, **Sz. Pál**, I. Antal:
   Design of oral sustained release delivery system by a melt dispersion method
   6th Central European Symposyum on pharmaceutical technology and biotechnology, Siófok, 2005.

3. A. Dévay, **Sz. Pál**, I. Antal:
   Formulation of sustained release diclophenac microcapsules
   6th Central European Symposyum on pharmaceutical technology and biotechnology, Siófok, 2005.

4. **Sz. Pál**, K. Mayer, A. Bodor, S. Nagy, A. Dévay:
   Evaluation of dissolution profiles of polyethyleneglycol and hydroxy propyl methyl cellulose based matrix tablets
   6th Central European Symposyum on pharmaceutical technology and biotechnology, Siófok, 2005.

5. A. Dévay, B. Kocsis, **Sz. Pál**, A. Bodor, K. Mayer, S. Nagy:
   New method for microbiological detection of delivery process from dosage forms containing antibiotics
   6th Central European Symposium on pharmaceutical technology and biotechnology, Siófok, 2005.

6. A. Dévay, **Sz. Pál**, K. Mayer, I. Klebovich, I. Antal:
   Study on pellet characteristics related to process parameters during high shear granulation
   Proceedings of the 1st BBBB Conference on Pharmaceutical Sciences, Siófok, 2005.

7. A. Dévay, K. Mayer, S. Nagy, **Sz. Pál**:
   Determination of particle size distribution of lipoid based pharmaceutical microstructures using dynamic light scattering
   8th Symposium on Instrumental Analysis, Graz, 2005.

8. A. Dévay, **Sz. Pál**, S. Nagy, K. Mayer, A. Bodor:
   Effects of pharmaceutical excipients in dosage forms containing N-acetycysteine (NAC)
   Pharmacy: Smart Molecules for Therapy,
   Magyar Tudományos Akadémia, Budapest, 2005.

9. A. Dévay, **Sz. Pál**, K. Mayer:
   Comparison of central composite factorial design and artificial neural networks on the evaluation of cochleate's size
   Pharmacy: Smart Molecules for Therapy,
   Magyar Tudományos Akadémia, Budapest, 2005.

10. A. Dévay, I. Antal, K. Mayer, **Sz. Pál**:
    Investigation of physical parameters of cochleates
    Gyógyszerkutatási Szimpózium, Pécs, 2005.

11. A. Dévay, S. Nagy, A. Bodor, K. Mayer, **Sz. Pál**:
    Application of Weibull distribution for investigation of controlled release matrix tablets
    Gyógyszerkutatási Szimpózium, Pécs, 2005.

12. I. Antal, J. Dredán, M. Lengyel, Á.Z. Dávid, **Sz. Pál**, I. Klebovich, A. Dévay:
    Prediction of dissolution profile stability based on diffuse reflectance spectra and solvent adsorption kinetics of coated pellets
    5th World Meeting on Pharmaceutics, Biopharmaceutics and Pharmaceutical Technology, Geneva, 2006.

13. A. Dévay, I. Antal, **Sz. Pál:**
    Investigation of process parameters on the size of lipid based nanostructures
    5th World Meeting on Pharmaceutics, Biopharmaceutics and Pharmaceutical Technology, Geneva, 2006.

14. **Sz. Pál**, A. Dévay:
    Ibuprofen tartalmú készítmények előállítása és vizsgálata
    Gyógyszerkutatási Szimpózium, Debrecen, 2006.

15. A. Dévay, **Sz. Pál**:
    Kohleátok előállítása és vizsgálata
    Gyógyszerkutatási Szimpózium, Debrecen, 2006.

16. A. Dévay, B. Kocsis, **Sz. Pál**, K. Mayer, S. Nagy:
    Experiments to decrease effect of incompatibility between povidone and ibuprofen in pharmaceutical dosage forms
    The 2nd BBBB Conference on Pharmaceutical Sciences,Tartu, 2007.

17. A. Dévay, S. Nagy, K. Mayer, **Sz. Pál:**
    Investigation of drug dissolution from cochleates applying transdermal diffusion cell
    The 2nd BBBB Conference on Pharmaceutical Sciences, Tartu, 2007.

18. A. Dévay, S. Nagy, K. Mayer, **Sz. Pál:**
Investigation of phosphatidylserine based nanostructures improving their stability in pharmaceutical dosage forms
The 2nd BBBB Conference on Pharmaceutical Sciences, Tartu, 2007.

19. A. Dévay, B. Kocsis, **Sz. Pál**, K. Mayer, S. Nagy:
Examination of dosage forms containing cephalexin by Microbiologically detected Dissolution
The 2nd BBBB Conference on Pharmaceutical Sciences, Tartu, 2007.

20. A. Dévay, B. Kocsis, **Sz. Pál**, K. Mayer, S. Nagy:
Az ibuprofen és a PVP inkompatibilitásának csökkentése co-freeze drying módszerrel
Gyógyszerkutatási Szipózium, Szeged, 2007.

21. A. Dévay, B. Kocsis, **Sz. Pál**, K. Mayer, S. Nagy:
Direkt tablettázással készült cefalexin tabletták hatóanyag-leadásának tanulmányozása különböző pH-n, mikrobiológiailag detektált kioldódás (MDD) vizsgálattal
Gyógyszerkutatási Szipózium, Szeged, 2007.

22. **Sz. Pál**, T. Bozó, A. Dévay:
Mesterséges neurális hálózat alkalmazása multipartikuláris rendszerek optimalizálása céljából
Gyógyszerkutatási Szipózium, Szeged, 2007.

23. T. Bozó, **Sz. Pál**, K. Mayer, S. Merczel, A. Dévay:
Liposzómák hatóanyag-leadásának vizsgálata változó fiziológiás feltételek mellett
Gyógyszerkutatási Szipózium, Szeged, 2007.

24. A. Dévay, K. Mayer, T. Bozó, **Sz. Pál:**
Félszilárd gyógyszerkészítmények hatóanyag-leadása membrándiffúziós cella alkalmazásával
Gyógyszerkutatási Szipózium, Szeged, 2007.

25. A. Dévay, I. Antal, **Sz. Pál:**
Analysis of pelletizing in high-shear granulator applying digital acoustic signal detection
Biopharmaceutics and Pharmaceutical Technology, Barcelona, 2008.

26. T. Bozó, **Sz. Pál**, K. Mayer, S. Merczel, S. Nagy, A. Dévay:
Investigation of encapsulation efficacy of liposomes applying conductivity measurement, 6th World Meeting on Pharmaceutics
Biopharmaceutics and Pharmaceutical Technology, Barcelona, 2008.

27. I. Antal, N. Kállai, J. Dredán, E. Balogh, **Sz. Pál**, A. Dévay, I. Klebovich:
Understanding and controlling drug layering and coating process using neutral pellets
6th World Meeting on Pharmaceutics, Biopharmaceutics and Pharmaceutical Technology, Barcelona, 2008.

28. A. Dévay, **Sz. Pál:**
A hatóanyagleadás folyamatának új elméleti és gyakorlati megközelítése
Congressus Pharmaceuticus Hungaricus, Budapest, 2009.

29. Gy. Horváth, P. Molnár, J. Deli, L. Szente, T. Bozó, **Sz. Pál**, A. Dévay, M. Simonyi, Á. Kemény, K. Sándor, J. Szolcsányi, Zs. Helyes:
Karotinoidok hatásának vizsgálata neurogén gyulladásos folyamatokra in vivo egérmodellekben
Congressus Pharmaceuticus Hungaricus, Budapest, 2009.

30. S. Merczel, **Sz. Pál**, B. Kocsis, A. Dévay:
Műkönnyek gyógyszertechnológiai optimalizálása és mikrobiológiai stabilizálása biokompatibilis gyógyszerkészítmény tervezése céljából
Congressus Pharmaceuticus Hungaricus, Budapest, 2009.

31. **Sz. Pál**, K. Mayer, S. Nagy, A. Dévay:
Granulátumok és pelletek folyási tulajdonságainak jellemzése képanalizáló módszer alkamazásával
Congressus Pharmaceuticus Hungaricus, Budapest, 2009.

32. K. Mayer, O. Pelczéder, **Sz. Pál**, A. Dévay:
Polivinil-alkohol tartalmú, biokompatibilis szemcsepp formulálása
Congressus Pharmaceuticus Hungaricus, Budapest, 2009.

33. A. Dévay, T. Pernecker, **Sz. Pál:**
Hipertenzív krízis kezelésére alkalmas multipartikuláris hatóanyag-leadó rendszer előállítása és vizsgálata,
Congressus Pharmaceuticus Hungaricus, Budapest, 2009.

34. A. Dévay, **Sz. Pál**, S. Nagy, K. Mayer:
Kisgép a receptúrában: félszilárd gyógyszerkészítmények receptúrai elkészítésének optimalizálása
Congressus Pharmaceuticus Hungaricus, Budapest, 2009.

35. A. Dévay, **Sz. Pál:**
Kronoterápiás gyógyszerhordozó rendszerek alkalmazhatóságának biofarmáciai és gyógyszertechnológiai szempontjai
XVI. Gyógyszertechnológiai Konferencia és VIII. Gyógyszer az ezredfordulón Konferencia, Siófok, 2010.

36. **Sz. Pál**, A. Dévay:
Dinamikus képanalizáló módszer gyógyszeres szemcsék folyási tulajdonságainak meghatározására
XVI. Gyógyszertechnológiai Konferencia és VIII. Gyógyszer az Ezredfordulón Konferencia, Siófok, 2010.

37. S. Merczel, K. Mayer, T. Bozó, **Sz. Pál**, A. Dévay:
Műkönnyek gyógyszertechnológiai optimalizálása es mikrobiológiai stabilizálása biokompatibilis gyógyszerkészítmény tervezése céljából
XVI. Gyógyszertechnológiai Konferencia és VIII. Gyógyszer az ezredfordulón Konferencia, Siófok, 2010.

38. A. Dévay, **Sz. Pál:**
Nanoméretű gyógyszerhordozó rendszerek fejlesztésének szempontjai
XVI. Gyógyszertechnológiai Konferencia és VIII. Gyógyszer az ezredfordulón Konferencia, Siófok, 2010.

39. **Sz. Pál**, A. Dévay:
Mikropelletek fizikai tulajdonságai és a szemcsék folyási sajátságai közti összefüggések feltárása dinamikus képanalizáló módszer alkalmazásával
XVI. Gyógyszertechnológiai Konferencia és VIII. Gyógyszer az ezredfordulón Konferencia, Siófok, 2010.

40. T. Pernecker, **Sz. Pál**, A. Dévay:
Bioadhezív segédanyagot tartalmazó szublingvális minitabletták előállításának optimalizálása hipertenzív krízis kezelése céljából
XVI. Gyógyszertechnológiai Konferencia és VIII. Gyógyszer az ezredfordulón Konferencia, Siófok, 2010.

41. S. Merczel, K. Mayer, **Sz. Pál**, A. Dévay:
Antimikrobás hatású szemészeti in situ hatóanyag-leadó rendszer kvantitatív vizsgálata
XVI. Gyógyszertechnológiai Konferencia és VIII. Gyógyszer az ezredfordulón Konferencia, Siófok, 2010.

42. K. Mayer, **Sz. Pál**, A. Dévay:
A gyógyszertári gyógyszerkészítés lehetőségei a korszerű terápiában
XVI. Gyógyszertechnológiai Konferencia és VIII. Gyógyszer az ezredfordulón Konferencia, Siófok, 2010.

43. A. Fittler, B. Brachmann, **Sz. Pál**, A. Dévay, B. Kocsis, Z. Matus, L. Botz:
Új utakon a gyógyszerforgalmazás? Az interneten rendelt gyógyszerek átfogó gyógyszerészeti vizsgálatai.
XVI. Gyógyszertechnológiai Konferencia és VIII. Gyógyszer az ezredfordulón Konferencia, Siófok, 2010.

44. Gy. Horváth, É. Szőke, P. Molnár, L. Szente, Á. Kemény, J. Deli., T. Bozó, **Sz. Pál**, A. Dévay, M. Simonyi, J. Szolcsányi, Zs. Helyes:
Inhibition of Mustard Oil-Induced Neural Responses by RAMEB-Lutein in Different In Vitro and In Vivo Systems
15th International Cyclodextrin Symposium, Vienna, 2010.

Table of Contents

List of Abbreviations

ATCC	**A**merican **T**ype **C**ulture **C**ollection
API	**A**ctive **P**harmaceutical **I**ngredient
BCS	**B**iopharmaceutical **C**lassification **S**ystem
CPL	**C**arbo**P**o**L**®/carbomer
DOE	**D**esign **O**f **E**xperiment
EC	**E**thyl**C**ellulose
ED	**E**xperimental **D**esign
EDTA	**E**thylene**D**iamine**T**etraacetic **A**cid
FBMR	**F**ocused **B**eam **R**eflectance **M**easurement
GI	**G**astro**I**ntestinal
GIC	**G**astro**I**ntestinal **C**andidiasis
HEC	**H**ydroxy**E**thyl**C**ellulose
HIV	**H**uman **I**mmundeficiency **V**irus
MDD	**M**icrobiologically **D**etected **D**issolution
MDT	**M**ean **D**issolution **T**ime
MTT	3-(4,5-di**M**ethyl**T**hiazol-2-yl)-2,5-diphenyl**T**etrazolium bromide
NIR	**N**ear **I**nfrared
NIRS	**N**ear **I**nfrared **S**pectroscopy
NS	**N**ot **S**ignificant

RH	**R**elative **H**umidity
RPM	**R**otation **P**er **M**inute
RRSB	**R**osin-**R**ammler-**B**ennett-**S**perling
RSV	**R**elative **S**wept **V**olume
SEM	**S**canning **E**lectron **M**icroscope
S.D.	**S**tandard **D**eviation
$\boldsymbol{\tau}$, $\boldsymbol{\tau_D}$	Mean Dissolution Time (MDT)
$\boldsymbol{\tau_M}$	MDT based on microbiological examinations
$\boldsymbol{\tau_S}$	MDT based on spectrophotometric examinations
TLC	**T**hin **L**ayer **C**htomatography
UV	**U**ltra **V**iolet
VIS	**VIS**ible

1. Introduction

Optimization of the drug release of peroral dosage forms and adjusting it to the absorption window of the active ingredient is the fundamental point in the development of a new pharmaceutical product [1,2]. However, there may be different aspects in cases when local effect is required. In this type of therapy the concept of the dissolution of active ingredients should be revaluated [3]. The enhancement of the bioavailability according to the Biopharmaceutical Classification System (BCS) [4] cannot be applied invariably [6], since importance of the absorption and the permeability is minor. Conversely, there are other essential parameters which should be taken into account during the development of these preparations, including the adhesivity to the mucous membrane, large contact surface of the drug particles, the profile and the time of drug release [7]. Among several diseases, gastrointestinal candidiasis (GIC) [8] was chosen to formulate and optimize a medicinal product taking into consideration the enhancement of the bioavailability of local effect.

Application of pellets in this therapy offers even more advantages. They are suitable to optimize drug release by their particle size, coating thickness or material.

Pellets among multiparticulate dosage forms offer several advantages generally in the therapy related to safety and effectiveness of the medicinal product such as individual reproducibility of gastric emptying, more regular absorption, increasingly stable, predictable plasma levels and a reduced risk of high concentrations [9,10]. This basic concept of multiple-unit systems is the fact that the dose of the active ingredient is released by the individual subunits, and the functionality of the entire dose depends on the quality of the subunits [11]. Pellets are suitable for further processing in order to optimize drug release by combining different particle size fractions and coating thickness [12] in capsules or compressing them into tablet.

Manufacturing of pellets requires specialized equipments, technologies and excipients. Pellets are usually prepared by wet agglomeration of fine powders of active ingredient and excipients into spherical units in closed granulating systems, i.e. in rotor-fluid granulators or high-shear mixers [13]. To produce pellets in a high shear mixer, the process involves distinct phases: homogenization of powders, granulation, spheronization and drying. The primer nucleus of future pellets is formed by binder spraying and dispersing during the agitation. Being a multivariate process, it is important to identify and control the process variables, i.e. the appropriate agitation prevents the development of too large particles [14,15,76]. Since

agglomerates undergo densification as mixing and spraying, the process time is expected as a critical parameter influencing quality of pellets.

Although various experiments were drawn up to investigate the effect of the formulation variables on the physical characteristics of pellets, only a few reports can be found in the pharmaceutical literature investigating the large number of process variables together during the pelletization concerning both the physical properties of granules and the drug release profile of the dosage form [16].

Modelling the effect of process variables with factorial designs and analysis of the response surfaces is a powerful, efficient and systematic tool that shortens the time required for the development of pharmaceutical dosage forms and improves research and development work [20].

The objective of the dissertation is to offer an optimized pharmaceutical preparation for the therapy of GIC containing *nystatin* to achieve a prolonged site-specific antifungal treatment using multiparticulate dosage form and special bioadhesive excipients based on preliminary examinations carried out on micropellets with model drug incorporated.

2. Aims

Aims of this research work are:

- determination of significant process variables and their effect of high-shear pelletization,
- application of the measurement of diffuse reflectance spectra as a possibility for fast in-process control during the pelletization process,
- application of optimized process variables in order to produce micropellets with specific physical characters for an optimized GIC therapy,
- application of Microbiologically Detected Dissolution (MDD) technique based on direct bioautography in order to determine the dissolution kinetics of antifungal substances,
- comparison of the MDD with other analytical method,
- optimizing the biopharmaceutical characters of micropellets for the antifungal action,
- recommendation of the manufacturing method and ingredients for a successful GIC therapy.

3. Literature survey

The literature survey of the thesis contains two parts. The first is concerned with the technological manufacture and optimization, the second part handles the therapeutic importance of locally acting micropellets.

Definition of pellets is not uniform, sometimes they are discussed together with granules and often the terms pellet-micropellet are not distinguished. Their preparation can be carried out in many ways with similarities to the preparation of granules [21]. According to the literature there are a few fix points which can characterize the pellet dosage form as spherical particles with almost smooth surface and compact texture independently to the method of preparation. If their size is below 1 mm, the term “micropellet”, between 1 and 2 mm, the term ”minipellet” can be used.

According to the structure, as seen on Fig. 1 we can distinguish pellets containing the API in the

1. matrix and in the
2. coating.

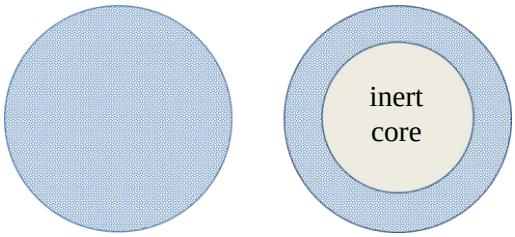

Figure 1. Basic types of pellets
(matrix pellet containing API on the left; inert pellet core with layer containing the API on the right)

Pellets have several pharmaceutical technological advantages, such as excellent flowability, easily optimizable particle size distribution, good mechanical stability, abrasion-resistant structure and optimizable coating due to the regular, uniform, smooth surface [13].

3.1. Interaction between particles, distribution of binder liquid

Interaction between solid particles during granulation was first scientifically investigated by *Rumpf* in the 50s [23]. In his work the following forces were listed:

1. attrition forces – gravitational force, magnetic force, electrostatic force or the van der Waal force play less role in the interactions between particles, than capillary forces,
2. solid bridges – they are developing during the formation of inorganic bonds, chemical reactions, crystallisation and melting phenomena,
3. shape closing bridges – they are developing due to the different shape and size of particles during pelletization getting into physical contact to each other,
4. liquid bridges – they are forming due to capillary forces which ensures the cohesion of particles and decrease the attrition forces.

Newitt and *Conway-Jones* distinguished four phases during the development of spherical particles according to the distribution of the binder liquid: the pendular state with liquid bridges, the funicular state in which the amount of liquid bridges increases capillary state and the droplet state [24].

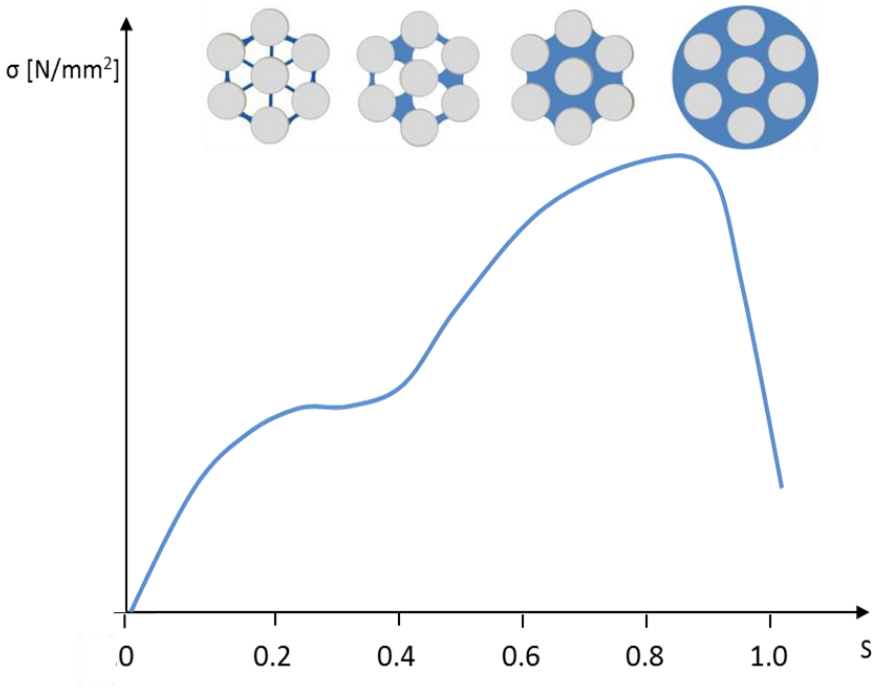

Figure 2. Stages of wetting (*S* means the liquid saturation level) and tensile strength (σ) during granulation

During pelletization right before the addition of any liquid small size particle-aggregates can be observed due to the secondary attrition forces. After the beginning of addition of liquid first drops start to connect the primary particles at the contact points. At the next, funicular stage, the liquid bridges may reach each other and more than two primary particles can be connected via this liquid bridge. Gaps are also started to be filled with liquid at this stage. At the next stage the structure of the pellet is formed and due to the capillary state the liquid added to the system is absorbed by the aggregated structure. The mechanical stability of the pellet is the highest at this point. Increasing the amount of the added liquid the droplet state can be reached, when the structure weakens and the system turns into paste or suspension.

Basically we can distinguish two types of binder liquid additions:

1. the size of the liquid drop is bigger than the size of the primary particle (drop addition),
2. the size of the liquid drop is smaller than the size of the primary particle (spray addition).

During the wetting of the powder mixture the contact angle (Θ) is the most important physical property which describes the wetting mechanism on the solid/liquid/gas boundary surface, which is the angle of solid/liquid and liquid/gas boundary surface.

We can distinguish:

1. contact wetting (Θ>0°),
2. film wetting (Θ=0°).

In case of Θ<90° we can state, that the substance is lyophilic, in case of Θ>90° it is lyophobic. After the equilibrium of solid/liquid/gas phases the relationship between the surface tension and the contact angle can be expressed by the *Young-Dupré* equation:

$$\gamma^{sv} - \gamma^{sl} - \gamma^{lv} \cos\Theta = 0 \qquad (1)$$

γ^{sv} solid/gas surface tension

γ^{sl} solid/liquid surface tension

γ^{lv} liquid/gas surface tension

Θ contact angle

Another way of characterisation of the wetting is the *Washburn*-test, which is based on the penetration of a liquid into a column filled with particles due to capillary forces. This phenomenon can be described by the following equation:

$$h_e - \frac{2\gamma^{lv}cos\theta}{\rho g R} = 0 \qquad (2)$$

h_e height of the liquid after the equilibrium

R average radius of capillaries in the particle agglomerate

ρ density of the liquid

g gravitational force

$\gamma^{lv}cos\Theta$ adhesion tension

3.2. Particle growth and attrition mechanism during pelletization

During pelletization the balance of particle growth and attrition mechanisms is very fundamental. We can distinguish four types of these mechanisms:

1. Nucleation – is the first step during particle growth, when primary particles are getting into contact to each other and stick together in the presence of the binder liquid forming a nucleus.
2. Coalescence – due to the collision of particles bigger aggregates are formed.
3. Layering – also called as „balling", when a larger amount of primary particles stick on the surface of a bigger aggregate due to liquid addition.
4. Breakage – there are more mechanisms for the breakage of granules/pellets:
    a. crushing – during which smaller granules or pellets crush and get onto the surface of bigger particles. There are several mechanisms of crushing:
        i. shattering,
        ii. fragmentation,

iii. abrasion,

b. abrasion transfer – during which the material transfer occurs between two colliding particles, while both particles stay intact.

These mechanisms are often described mathematically by different models according to different steps of pellet formation. Strength of liquid bridge between two colliding particles determines whether they stay intact or attach together. The greatest force which depends on the relative amount between two particles comparing to their volume was first described by *Rumpf* [23]:

$$F_{cap} = \alpha \gamma_l d_p \tag{3}$$

$1.9 < \alpha < \pi$ coefficient depending on the amount of moisture

γ_l surface tension of the liquid

d_p diameter of the particle

Rumpf described another relationship for the breakage of granules, which includes the particles tensile strength (σ_t) in funicular or capillar state:

$$\sigma_t = C \cdot S \cdot \frac{1-\varepsilon}{\varepsilon} \cdot \frac{\gamma_l}{d_{pp}} \cdot \cos\Theta \tag{4}$$

C coordination number dependent from the shape of the particle

S liquid saturation of the granule

ε intragranular porosity

d_{pp} diameter of the primary particle

Θ contact angle

Ouchiyama and *Tanaka* determined a model which can be used to calculate the critical diameter (d_c) above which there is no coalescence [25]:

$$dc = c \cdot \left(K^{3/2} \cdot \sigma_t \right)^a \tag{5}$$

a and c	constants
K	deformation constant
σ_t	tensile strength of the granule

The 'K' deformation constant can be described as the ratio of the contact surface (A) and the compaction force (F):

$$K = \frac{A}{F} \tag{6}$$

Kristensen et al completed *Ouchiyama* and *Tanaka's* model to calculate the tensile strength of the granule particles and stated that granule particles must reach a minimal mechanical stability for the coalescence [26].

Ennis et al recognized, that the viscosity of the liquid significantly influences the cohesion force of the liquid bridge, thus an agglomeration model was developed for the dynamic liquid bridge [28]. Depending on the kinetic energy during the collision of particles the energy spread across the system is used at coalescence or the reflexion of particles. To describe this system *Ennis* et al introduced the dimensionless viscous Stokes number:

$$St_v = \frac{8\rho_p v_0 r}{9\eta} \tag{7}$$

ρ_p density of the pellet/granule

v_0 relative velocity between two particles

r radius of the pellet/granule

η viscosity of the binder liquid

The viscous Stokes number is the ratio of two colliding particle's energy and the spreading of energy in a viscous binding liquid [29]. In case of a high-shear granulator the velocity of the collision is in direct proportion to the impeller rotation speed (v_{imo}):

$$v_{imo} = \pi ND \tag{8}$$

N rotating speed of the impeller

D diameter of the granulation bowl

Since in case of collision of two particles they lose kinetic energy, the velocity before the collision (v_0) is higher than the velocity after the collision (v).

Coalescence occurs when the viscous Stokes number (St_v) is smaller than its critical value (St_v^*):

$$St_v^* = \left(1+\frac{1}{e}\right)\ln\left(\frac{h}{h_a}\right) \tag{9}$$

e rearrangement coefficient, which can be calculated from the difference of velocity before and after the collision

h thickness of the liquid layer on the surface of the pellet

h_a surface roughness (diameter of the primary particles is also 'h_a')

According to the theory above there are three cases regarding the values St_v and St_v^*:

1. $St_v \ll St_v^*$ - in this case all collisions are successful
2. $St_v = St_v^*$ - some collisions are successful
3. $St_v \gg St_v^*$ - none of the collisions are successful

From the expressions above we can state, that the collision of the particles and growth by coalescence has higher probability at low particle density, low impeller speed, small particle size, high viscosity liquid binder, small rearrangement coefficient, thick surface liquid layer and smooth particle surface. Since these variables usually change in function of time, above calculations can only be used for retrospective studies.

3.3. Operation of pelletization

Similarly to the granules there are three main types of operations of pelletization:

1. **Solvent pelletization** – the applied liquid dissolves totally or partially one or more components of the powder mixture. During the addition of the liquid a saturated solution develops on the surface of the particles which binds them together. After the evaporation of the solvent the dissolved component gathers on the surface of the pellet and crystallizes, forming a thick coating (Fig.3.) [21].

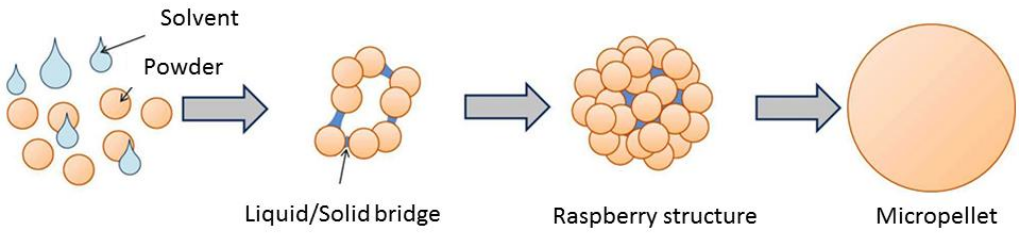

Figure 3. Mechanism of pelletizing with solvent

2. **Binder pelletization** – usually high molecular weight polymers are used. The powder mixture is usually wetted by the proper amount of binder liquid and then it is kneaded. The binder material also can be added in its powder form, but these pellets' mechanical properties are usually poor (Fig.4.) [21].

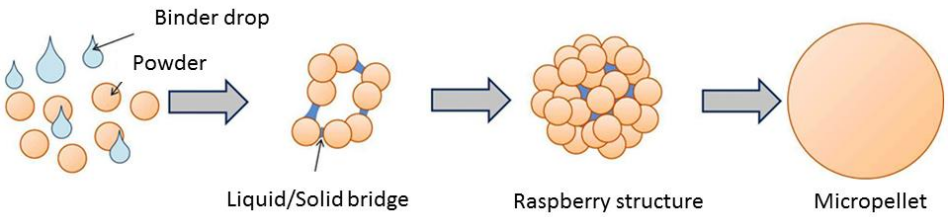

Figure 4. Mechanism of pelletizing with binding agent

3. **Sinter pelletization** – in this case one or more components of the powder mixture has a lower melting point (usually high molecular weight macrogol). Heating the mixture partial melting occurs. Spray drying or freeze drying this mixture result almost perfectly spherical pellets (Fig.5.) [21].

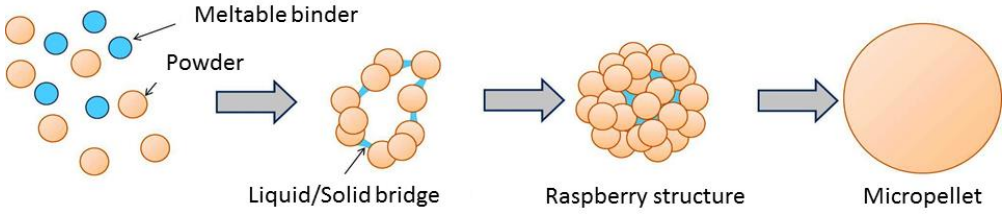

Figure 5. Mechanism of pelletizing with sintering

In order to carry out pelletizing, several procedures are available, which will be discussed in the following chapters.

3.3.1. Mixing method

This is the simplest way of pelletisation. This method usually results heterogeneous particle size distribution. During this method the powder mixture and the liquid binder both are placed into a rotating caldron, where the pellets are formed [13].

3.3.2. Rotary disk method

The powder mixture is placed on the surface of a rotating flat disk or a conical body, while the binder liquid is added from the centre of the rotating axis. Developing particles roll to the edge of the rotating disk due to the centrifugal force, during which they gain their spherical shape. Using this method spheronization of preliminary prepared granules can also be carried out (Fig.6.).

Figure 6. Rotary disk pelletizing equipment [77]

3.3.3. Extrusion-spheronization method

This is one of the most commonly used pellet preparation method [27]. Powder components are kneaded with the liquid, then the wet mass is extruded through a 0.5-2.0 mm diameter hole size disk. After this step the plastic and wet extrudate is spheronized (Fig.7.) [30].

Figure 7. Extruder during operation [77]

3.3.4. Roto-fluid method

Applying fluid-bed granulation, spheronization and drying is carried out in one complex step. There is a rotating disk at the bottom of the machine with a conical body in the centre (Fig. 8.). Due to the fluid air, the rotating disk and the conical body particles circulate around the wall of the working area and roll on the surface of the disk. The liquid is added towards the centre of the working space spraying the liquid to the rotational direction. Reaching the proper particle size the liquid addition is stopped and from this point only spheronization and drying is carried out. Roto-fluid pelletization is one of the most power consuming and expensive methods, its advantage is the high productivity and the one-step production [21].

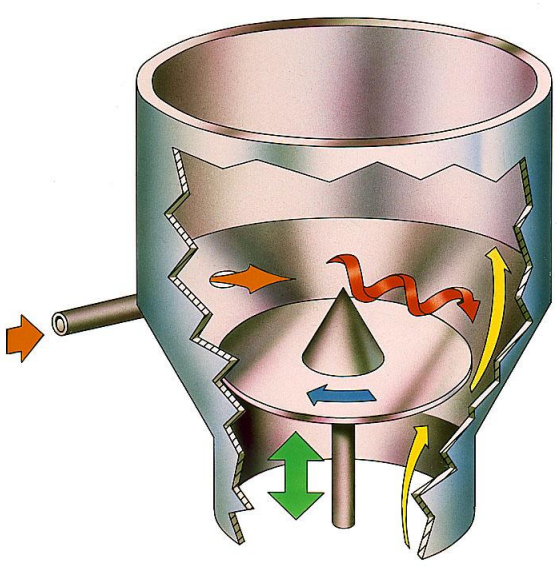

Figure 8. Operation of roto-fluid machine [77]

3.3.5. Spray drying and freeze drying

API is dispersed in the vehicle's solution, and then it is sprayed. Perfectly spherical droplets formed during this preparation are then dried by hot or cold air [21].

3.3.6. High-shear pelletization

This method unifies the main steps of the classic wet granulation (homogenization, wetting, kneading and particle forming) and the spheronization. The production is carried out in one working space similarly to the fluidisation in one complex step (Fig. 9.). During high-shear granulation intense mixing of the components and the presence of the shearing forces results the smooth and compact spherical particles. The mechanical parameters of the end-product depend on the operation variables. Spray or drop form of liquid is immediately dispersed due to the high rotation speed of mixer elements, thus reaching a quick and perfect wetting. Main mixer elements consists the impeller and the chopper. The impeller is at the bottom of the working space reaching rotation speed of 500-2000 rpm. The impeller moves the mass around the working space and in radial direction outwards from the centre to the wall. The mass produces a whirling movement and continuously falls back towards the centre. Chopper blades can be placed at the bottom, top or tangentially to the rotation axis of the impeller. This mixer element is composed of more smaller, thinner blades (3-6), which enhance the shearing forces during the production. Their speed also varies between 500-2000 rpm. Pellets produced in the high-shear machine can be dried by microwave or heating double-jacket as well. The production method is extremely quick, there is low risk of contamination due to the closed working area. Choosing the proper operation variables and applying the proper excipients almost all pharmaceutical technological and biopharmaceutical parameters can be optimized and controlled [13].

Most important variables during high-shear production related to the equipment:

1. mixing bowl
    a. shape
    b. size
    c. material
2. impeller
    a. shape
    b. size
    c. speed
3. chopper
    a. shape
    b. size
    c. speed
4. temperature of the working space
5. operation time

Most important variables during high-shear production related to the material are:

1. powder composition (particle size distribution, physical properties)
2. weight
3. liquid binder
    a. viscosity
    b. density
    c. amount
    d. dosing speed
    e. dosing method

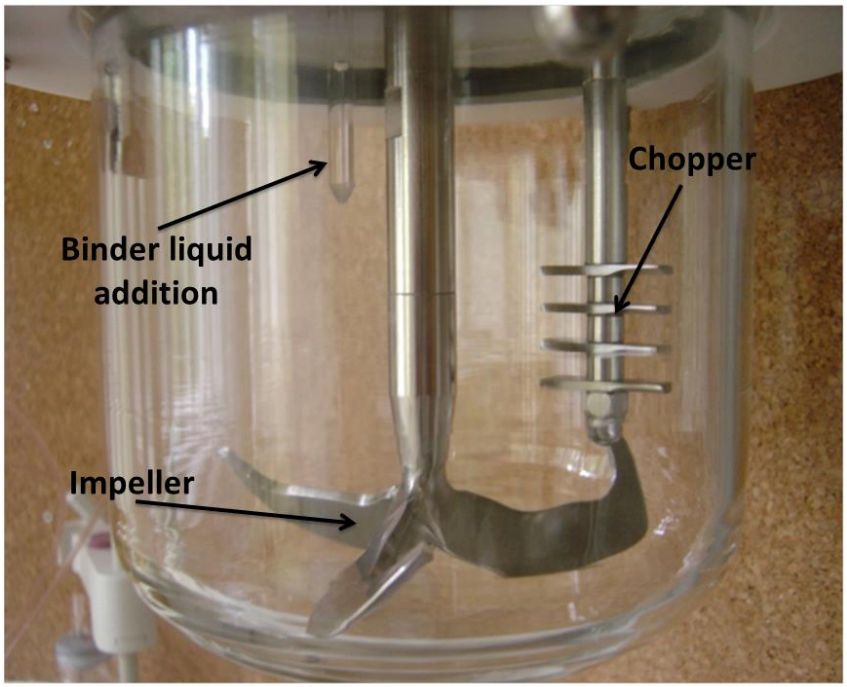

Figure 9. Lab-scale high share granulator (Pro-C-epT 4M8, Belgium, Zelzate)

3.3.6.1. Forces during high-shear pelletization

During pelletization presence and equilibrium of integration and reduction effects leads to the formation of pellets, which are based on the following forces:

- gravitational force
- acceleration force
- centrifugal force
- resistance of the pelletizing bowl
- fluid effects developed by the impeller

For the characterisation of the forces effecting the preparation, the tip speed of the impeller is commonly used, which is directly proportional to its shearing force. The perimetric speed is responsible for the movement of the wet mass. This value can be calculated by the following expression:

$$v_t = v_f \, 2 \, \pi \, r \qquad (10)$$

v_t velocity of the tip of the impeller

v_f speed of the rotor of the impeller (rpm)

r radius of the circle done by the tip of the impeller

The Froude number describes the forces affecting to the wet mass resulting its compaction, which is carried out by the impeller. The *Froude* number is a dimensionless value.

$$Fr = \frac{v^2 r}{G} \tag{11}$$

Fr Froude number

v speed of the impeller

r radius of the circle done by the tip of the impeller

G acceleration of gravity

At smaller, laboratory production scale the Froude number is usually higher, than in industrial scale. The higher number means bigger pellet size, more compact structure, which can result the cohesion of the particles to the pelletizing bowl [33].

3.3.6.2. Determination of end-point of high-shear pelletization

Critical point of the high-shear pelletization is the determination of the end-point of the production. The end-point is usually determined by the technologist according to the particle size, the particle size distribution, density, and the powder rheology. Instrumented high-shear machines have several parameters which are observed in order to forecast and determine the optimal end-point [34].

Most important methods include:

- measurement of power consumption,
- measurement of the impeller torque,
- other methods based on the measurement of the impeller torque,
- alternative measurement methods.

3.3.6.2.1. Measurement of power consumption

One of the most commonly used methods is the measurement of the power consumption of the impeller. Scientific literature several times reported that the increase of the pellet size has close correlation to the increasing power consumption. This correlation is not linear, but it is characteristic and reproducible to the definite powder composition [35].

3.3.6.2.2. Measurement of the impeller torque

The second most commonly used method is the measurement of the impeller torque, which has good correlation to the previously mentioned method, since sometimes it is recommended to use the more complex measurement of the impeller torque due to insensitivities in the power consumption profile in case of definite weight of mass or other specific parameters. The profile of the impeller torque divides the pellet formation process into five phases. In the first phase the powder is moistened without forming liquid bridges. In the second phase liquid bridges are formed between the particles and first granules are formed. Formation of coarse

agglomerates could be observed in the third phase and in the fourth phase large areas are filled with liquid. In the fifth phase when the liquid saturation equals 100%, the system becomes a suspension [35]. The end-point of the pelletization is usually during the fourth phase.

3.3.6.2.3. Other methods based on the measurement of impeller torque

- **Torque rheometer method** – the third most commonly used method, which also provides information on rheological properties [38].
- **Torque reaction force method** – applies Newton's third law of action-reaction. During the measurement the rotor tries to move against the rotational direction which develops forces inside the engine, which can be detected and used for the end-point determination [35].

3.3.6.2.4. Alternative measurement methods

There are several other measurement methods supplementing the lacks of the methods mentioned above:

- **Application of NIR sensor** – this method is based on the moisture changes of the particles. Its disadvantage is that the sensor can only detect the moisture on the surface of the wet mass [39]].
- **Focused Beam Reflectance Measurement (FBMR)** – the method is based on the particle size determination. This method cannot be used for end-point determination alone, but it can be a perfect supplement of other methods [40].
- **Acoustic sensor measurement** – one of the oldest methods of the end-point determination which can be used alone and as a supplementing tool as well. Development of the technology in recent years and modern analysis softwares provide more potential to this method [31].

3.4. Biopharmaceutical background

Gastrointestinal candidiasis (GIC) often occurs in patients suffering from immunosuppression (e.g. related to HIV infection), but many researchers found GIC also in non-immuno suppressed humans. GIC belongs to one of the most discussed diseases, since it is still undecided whether it can cause systemic symptoms or not. Researches, however, indicate GIC diseases may be more prevalent than it is supposed. Several antifungal pharmaceutical ingredients are considered to be effective in the therapy of GIC as listed in Table I [43].

Table I. BCS classification of antifungal agents used in candidiasis

BCS Class	Antifungal agent	Biopharmaceutical properties
1	-	high solubility, high permeability
2	*clotrimazole, itraconazole*	low solubility, high permeability
3	*fluconazole, capsofungin*	high solubility, low permeability
4	*amphotericin B, nystatin*	low solubility, low permeability

Clotrimazole (Fig. 10.) belongs to the group of imidazoles, it is applied in 10 mg troches 5 times a day in mucosal candidiasis. According to the Ph. Eur. 8. it is white or pale yellow crystalline powder. It is practically insoluble in water; soluble in alcohol, in acetone, in chloroform, and in methyl alcohol [44].

$C_{22}H_{17}ClN_2 = 344.8$

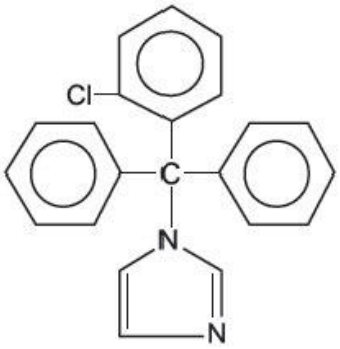

Figure 10. Structural formula of *clotrimazole,* 1-(α -2-Chlorotrityl)imidazole

Itraconazole (Fig. 11.) is a triazole antifungal ingredient applied in oral solution 200 mg/day. This substance is a white powder, insoluble in water; very slightly soluble in alcohol; freely soluble in dichloromethane; sparingly soluble in tetrahydrofuran [44].

$C_{35}H_{38}Cl_2N_8O_4$ = 705.6

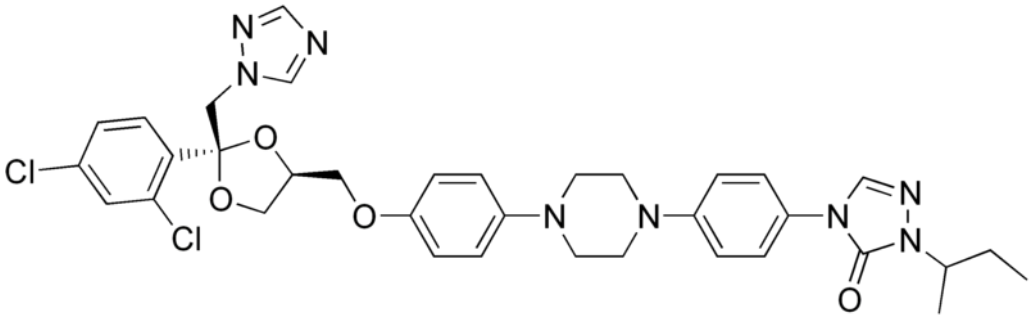

Figure 11. Structural formula of *itraconazole*, (±)-2-*sec*-Butyl-4-[4-(4-{4-[(2*R**,4*S**)-2-(2,4-dichlorophenyl)-2-(1*H*-1,2,4-triazol-1-ylmethyl)-1,3-dioxolan-4-ylmethoxy]phenyl}-piperazin-1-yl)phenyl]-2,4-dihydro-1,2,4-triazol-3-one

Fluconazole (Fig. 12.) is also a triazole antifungal ingredient applied in 100-200 mg. It is a white or almost white, hygroscopic, crystalline powder, slightly soluble in water; freely soluble in methyl alcohol; soluble in acetone [44].

$C_{13}H_{12}F_2N_6O$ = 306.3

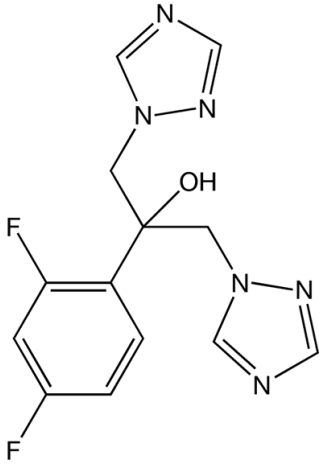

Figure 12. Structural formula of *fluconazole*, 2-(2,4-Difluorophenyl)-1,3-bis(1*H*-1,2,4-triazol-1-l)propan-2-ol

Capsofungin (Fig. 13.) is a β-3-glucan synthase inhibitor applied in 50 mg i.v. dose [44].

$C_{52}H_{88}N_{10}O_{15}$, $2C_2H_4O_2$ = 1213.4

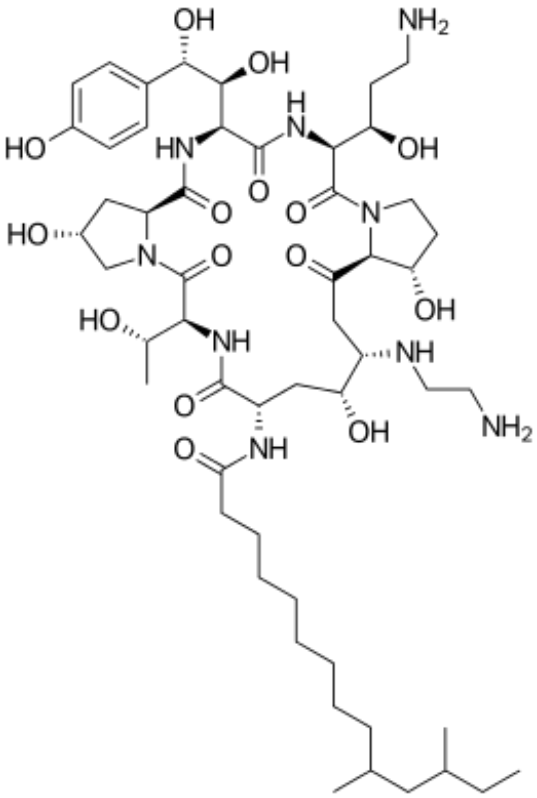

Figure 13. Structural formula of *capsofungin*, (4R,5S)-5-[(2-Aminoethyl)amino]-N2-(10,12-dimethyltetradecanoyl)-4-hydroxy-L-ornithyl-L-threonyl-trans-4-hydroxy-L-prolyl-(S)-4-hydroxy-4-(p-hydroxyphenyl)-L-threonyl-threo-3-hydroxy-L-ornithyl-trans-3-hydroxy-L-proline cyclic (6→1)-peptide diacetate

Amphotericin B (Fig. 14.) yellow or orange powder, which is a mixture of polyene antifungal ingredients, produced by the growth of certain strains of *Streptomyces nodosus.* It is practically insoluble in water and in alcohol; soluble in dimethyl sulfoxide and in propylene glycol; slightly soluble in dimethylformamide; very slightly soluble in methyl alcohol [44]. 100mg/ml oral suspension is also applied, though due to its absorption severe side effects might occur as well as in case of other effective antimicrobial substances, since the high concentration of the applied antifungal agents may develop severe side effects [45].

$C_{47}H_{73}NO_{17}$ = 924.1

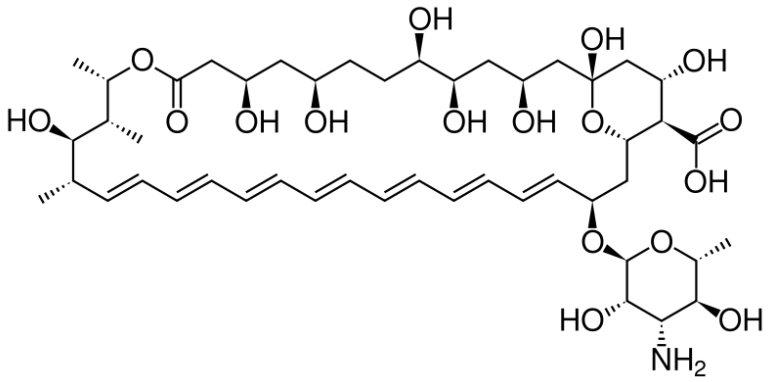

Figure 14. Structural formula of *amphotericin B*, (1*R*,3*S*,5*R*,6*R*,9*R*, 11*R*,15*S*,16*R*,17*R*,18*S*,19*E*,21*E*, 23*E*,25*E*,27*E*,29*E*,31*E*,33*R*,35*S*,36*R*,37*S*)- 33-[(3-amino- 3,6-dideoxy- β-D-mannopyranosyl)oxy]-1,3,5,6,9,11,17,37-octahydroxy- 15,16,18-trimethyl- 13-oxo- 14,39-dioxabicyclo [33.3.1] nonatriaconta-19,21,23,25,27,29,31-heptaene- 36-carboxylic acid

Pharmaceutical character of *nystatin* will be summarized later in chapter 4.1.1. Its effect is based on the topical action and the contact time with the mucous membrane, thus the formulation should adhere to the affected area as long as possible, however available dosage forms are unable to achieve an optimized effect, lacking the specialities of the adequate topical treatment. To reach this aim, mucoadhesive materials are needed to be added. Application of mucoadhesive polymers in the formulation, such as the anionic carbomer (CPL) and the non-ionic hydroxyethylcellulose (HEC) is a possible method for the targeted mucosal drug delivery which has been introduced to the pharmaceutics in the late 1960s [48].

In our study after preliminary examinations of high-shear granulation, *nystatin* was chosen as one of the most adequate API for the treatment of GIC due to its preferential properties [43]. Micropellets containing *nystatin* with increased specific surface were produced according to an experimental design containing bioadhesive excipients, which can prolong the contact time with the mucous membranes. The pellet size and the proportion of bioadhesive substances (carbopol®/hydroxyethylcellulose) were taken into consideration as variables affecting the therapy [51].

During the evaluation, in vitro spectrophotometrical, microbiological dissolution, ex vivo bioadhesion and swelling tests were carried out.

Effectiveness of the produced medicament samples was evaluated by the determination of the drug release [52]. Developing possibilities of *nystatin* determination methods are continuing intensively, since classic UV analytical methods in the pharmaceutical practice are not suitable to follow exact changes of antifungal activity of *nystatin* [53]. UV spectrum of *nystatin* demonstrates three main local maxima at 290, 306 and 318 nm which are only reliable at the same molecular state. Micellar structure of the polyene *nystatin* can lead to differences in the UV spectrum [54]. Numerous colour reactions were also tested, but there was no confirmed correlation with the biological activity [55]. A generalized assumption was later published regarding the lack of relationship for all polyene antibiotics between the UV spectrophotometric assay and the biological activity, which eventuated to include an agar diffusion method for the quantitative assay of *nystatin* in the Ph. Eur. 5. However, the agar diffusion method is sometimes time, cost and power consuming especially in case of large quantity of samples. Application of thin layer chromatography (TLC) based direct bioautography during the drug dissolution tests, microbiologically detected dissolution (MDD) can be carried out [56]. The MDD does not need strict sterile conditions and it is almost 100 times more sensitive than the agar diffusion method. Novel approach to enhance the UV spectrophotometric determination and to achieve better correlation is the application of the third-derivative spectrophotometric evaluation, which was applied in our experiments. The objective of the present study is to offer an optimized drug formulation by revealing the relationship between average pellet size, CPL and HEC content and optimized drug release to achieve a site-specific antifungal therapy.

4. Materials and Methods

4.1. Materials

4.1.1. Nystatin

The polyene antifungal antibiotic *nystatin* (Fig. 15.) (BCS class IV.) is one of the most important active agents in the site-specific treatment of the candidiasis [46], as it was reported by several clinical researches. *Nystatin* is a yellow or slightly brownish hygroscopic substance obtained by fermentation using the ATCC 11455 strain of Streptomyces noursei [44]. *Nystatin* is very poorly absorbed from the gastrointestinal tract, therefore the development of side effects is suppressed. It is excreted almost entirely in the faeces.

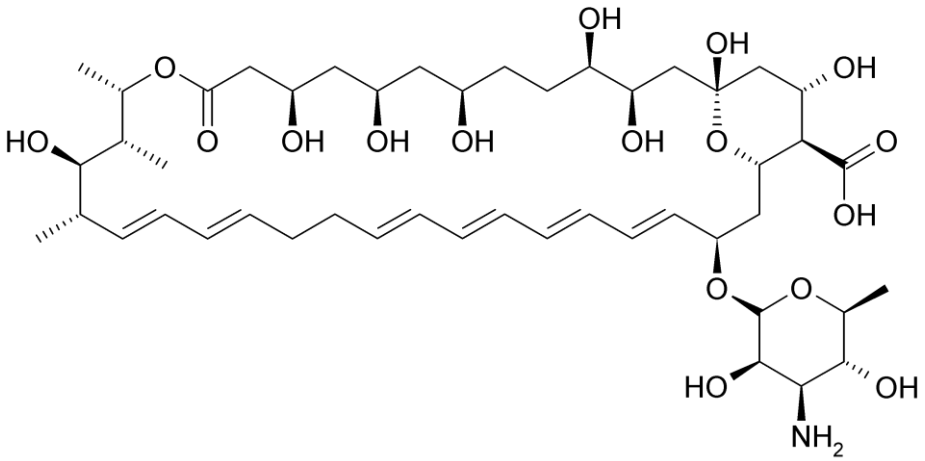

Figure 15. Structure of *nystatin*, (1*S*,3*R*,4*R*,7*R*,9*R*,11*R*,15*S*,16*R*,17*R*,18*S*,19*E*,21*E*, 25*E*,27*E*,29*E*,31*E*,33*R*,35*S*,36*R*,37*S*)-33-[(3-amino-3,6-dideoxy-β-L-mannopyranosyl)oxy]-1, 3,4,7,9,11,17,37-octahydroxy-15, 16,18-trimethyl-13-oxo-14, 39-dioxabicyclo[33.3.1]nonatriaconta-19, 21,25,27,29,31-hexaene-36-carboxylic acid

4.1.2. Pharmaceutical excipients

4.1.2.1. Microcrystalline cellulose

Microcrystalline cellulose is purified, partially depolymerized cellulose that occurs as a white, odourless, tasteless, crystalline powder composed of porous particles. Microcrystalline cellulose is widely used in pharmaceuticals, primarily as a binder/diluent in oral tablet and

capsule formulations where it is used in both wet-granulation and direct-compression processes [36]. In our experiments Avicel PH 101 and Avicel PH 105 were used.

4.1.2.2. α-lactose-monohydrate

Lactose occurs as white to off-white crystalline particles or powder. It is odourless and slightly sweet-tasting; the lactose is approximately 20% as sweet as sucrose. This excipient is widely used as a filler or diluent in tablets and capsules [36].

4.1.2.3. Ethylcellulose

Ethylcellulose (EC) is a tasteless, free-flowing, white powder. Ethylcellulose is widely used in oral and topical pharmaceutical formulations. The main use of ethylcellulose in oral formulations is as a hydrophobic coating agent for tablets and granules. Ethylcellulose coatings are used to modify the release of a drug) to mask an unpleasant taste, or to improve the stability of a formulation; for example, where granules are coated with ethylcellulose to inhibit oxidation. Modified release tablet formulations may also be produced using ethylcellulose as a matrix former [36].

4.1.2.4. Hydroxyethylcellulose

Hydroxyethylcellulose (HEC) occurs as a light tan or cream to white colored, odorless and tasteless, hygroscopic powder. Hydroxyethylcellulose is a non-ionic, water-soluble polymer widely used in pharmaceutical formulations, primarily used as a thickening agent in ophthalmic and topical formulations. It is also used as a binder and film-coating agent for tablets as well as an excipient for its bioadhesive properties [36].

4.1.2.5. Carbomer

Carbomers (CPL) are white-colored, acidic, hygroscopic powders with a slight characteristic odour. Carbomers are synthetic high-molecular-weight polymers of acrylic acid that are cross-linked with either allyl sucrose or allyl ethers of pentaerythritol. They are mainly used in liquid or semisolid pharmaceutical formulations as suspending or viscosity-increasing agents.

Formulations include creams, gels, and ointments for use in ophthalmic, rectal and topical preparations. It is also used as a bioadhesive material in oral preparations [36].

4.2. Methods

4.2.1. Design of experiments

Design, operation and control of pharmaceutical technological systems are based on information and their processing. Understanding of procedures is carried out by data mining, which means knowledge discovery from a database. Data mining is a scientific action, which aims at discovery of particular phenomena and procedures by data management and search and analysis of their correlations.

Afterwards discovery of procedures (process analysis) will take place the control of procedure, which can only be efficient, if factors can be determined, which are influencing quality parameters. The factors can be grouped accordingly how extent and in which way are able to effect on particular parameters.

One of the most important tasks of experimental design is the optimization of a preparation, which can be defined as search of the best and most favourable values of a phenomenon in order to create the necessary technological conditions. Size of manufacture batch, manufacturing time and particular operation parameters can also be obtained by optimization of parameters [58].

With the usage of factorial experimental design, few numbers of experiments are enough to explore the correlation between independent and dependent variables. Requirements of chosen parameters and factors are:

- controllability,
- accuracy,
- factor has to be unambiguous and directed to the particular object,
- independence between factors.

The experimental design (ED, or Design of Experiment, DOE) means plan or design containing settings and sequence, which has to be compiled even before beginning of experiment. This is an effective method, which allows planning and analysis of experiments,

objective evaluation of obtained result, conclusion, after which follow the steps for optimization of particular process.

Full factorial experimental design is regarded if all possible factor level combination and fractional factorial experiments are performed. If just a part of the full, partial factor design is carried out. Latter one can significantly reduce the necessary number of experiments, which should be performed.

The linear model

for two factors (x_1 and x_2):

$$Y = b_o + b_1 x_1 + b_2 x_2 + b_{12} x_1 x_2 \qquad (12)$$

b coefficient

$x_1 x_2$ interactions

for three factors (x_1 , x_2 and x_3):

$$Y = b_o + b_1 x_1 + b_2 x_2 + b_3 x_3 + b_{12} x_1 x_2 + b_{13} x_1 x_3 + b_{23} x_2 x_3 + b_{123} x_1 x_2 x_3 \qquad (13)$$

b coefficient

$x_1 x_2$, $x_1 x_3$, $x_2 x_3$, $x_1 x_2 x_3$ interactions

Mathematic model determined experimentally is appropriate to describe or characterize an examined system, if it meets with the criteria of adequacy. Namely there is no significant difference between output of system calculated according to computer and output of actual system.

Optimization can be performed by applying the gradient descent method developed by *Box and Wilson*. The principal of this method is that in order to determine the optimum, simultaneous change of significant factors is required [59].

4.2.2. Preliminary studies for high-shear pelletization

Among the available methods of preparation high-shear granulation was chosen to produce pellets. In order to determine significant process parameters of high-shear granulation, pellets were prepared containing anhydrous theophylline as model drug, α-lactose monohydrate, microcrystalline cellulose and ethylcellulose. Quality of all materials used in the experiments was Ph. Eur. 5. The powders were loaded into the bowl and premixed for 3 min.

During the pelletization the amount of the purified water used as granulation liquid was the amount of 45% calculated on the loaded mass. The binder flow time was kept constant at 5 minutes.

After production, pellets were dried to constant weight at 35°C, and stored at 25 °C, 60% RH in closed containers until their evaluation.

The high shear pelletization process was performed in a Pro-C-epT 4M8 granulator (Zelzate, Belgium). During the production two process variables were chosen to be investigated defined as factors [59]:

– impeller speed (x_1),
– binder flow rate (x_2).

Chopper speed was constant kept at 2000 rpm. An experimental design was carried out to reduce the number of experiments needed to obtain the highest amount of information on product and the effect of manufacturing process variables. The trials were carried out in triplicate in a randomized order. The variation intervals of independent variables and their coded levels are detailed in Table II. First, to find the most powerful process parameters, a 3-level face-centred central composite experimental design was conducted assuming a second order polynomial model according to the matrix demonstrated by Table III. The highest order of interaction (x_1x_2) was chosen as design generator to minimize the alias of coefficients through the defining contrast.

Table II. Independent process variables: factors and their coded levels

Factors	**Variation intervals**		
	Low (− 1)	**Base (0)**	**High (+ 1)**
x_1 impeller speed (rpm)	500	750	1000
x_2 binder flow (ml/min)	8	10	12

Table III. 2-factor, 3-level face centred central composite experimental design matrix for the pelletization

Trial	**Controlled factor**	
	x_1 **Impeller speed (rpm)**	x_2 **Binder flow (ml/min)**
1	1000	12
2	500	12
3	1000	8
4	500	8
5	1000	10
6	500	10
7	750	12
8	750	8
9	750	10

4.2.2.1. Determination of end-point of pelletization

Measurement of the impeller torque was used for the determination of pelletization end-point. It is a prevalent technique due to its reliability and in-process possibilities. The principle of this method is the detection of the resistance caused by the wet mass obstructing the impeller's movement. End-point was determined according to the profile of the impeller torque during production in the IV. phase of high-shear granulation (see Chapter 3.3.6.2.2.).

4.2.3. Manufacture of micropellets containing *nystatin* for application GIC therapy

Nystatin (Merck, Darmstadt, Germany), α-lactose-monohydrate (DC, BDI, Zwolle, Netherlands), microcrystalline cellulose (Avicel PH 105, FMC, Philadelphia, USA), hydroxyethylcellulose (HEC) (Hercules, Wilmington, USA) and carbomer (CPL) (Carbopol 934P, Hercules, Wilmington, USA) were used to prepare pellets. Purified water was used as granulation liquid. Quality of all materials used in the experiments was Ph. Eur. 7.

Pellets were produced in a high-shear mixer (Pro-C-epT 4M8 Granulator, Belgium, Zelzate) with a three-blade impeller and a chopper. Each batch contained 5% *nystatin*, 45% microcrystalline cellulose, hydroxyethylcellulose and carbomer in different amounts (0-5%) according to an experimental design, α-lactose-monohydrate added as diluent so that the total dry mass was 100.0 g. Powders were loaded into a 1000 ml bowl and premixed for 3 minutes. Purified water was used as binder liquid.

Pellets of 15 samples were prepared according to a central composite factorial design (Table IV. and V.) in triplicate. Experimental design of full type with five centre points had three numeric factors including average pellet size (x_1), CPL (x_2) and HEC (x_3) content and five coded levels (-1.414, -1, 0, +1, +1.414). Different average pellet sizes with various CPL and HEC contents were produced in the trials in order to examine different preparations. During statistical evaluations Design Expert v.7.0 (Stat-Ease Inc., Minneapolis, USA) was used to calculate the relative effect of factors (b), the confidence interval was 95%, significance was determined if $p<0.05$. TableCurve® 3D v. 4.0 (Systat Software Inc., London, UK) was used to reveal the response surface from the polynomial equation calculated using the experimental design.

An Erweka vibrating sieve (Erweka GmbH, Heusenstamm, Germany) had been used for determining pellet size and separation of pellets by average size, according to the experimental design.

Table IV. Central composite factorial design with two level factorial design points (-1,1), axial points (-1.414, 1.414) and a centre point (0)

Trial	x_1	x_2	x_3
1	1	1	-1
2	1	-1	1
3	-1	1	1
4	-1	-1	-1
5	-1.414	0	0
6	1.414	0	0
7	0	-1.414	0
8	0	1.414	0
9	0	0	-1.414
10	0	0	1.414
11	0	0	0
12	0	0	0
13	0	0	0
14	0	0	0
15	0	0	0

Table V. Process parameters of trials

Factors with coded levels	**-1.414**	**-1**	**0**	**1**	**1.414**
x_1, average pellet size (μm)	217.2	300.00	500.00	700.00	782.8
x_2, CPL content (g)	0.00	0.73	2.50	4.27	5.00
x_3, HEC content (g)	0.00	0.73	2.50	4.27	5.00

4.2.4. Examinations of pellets

4.2.4.1. Particle size analysis

The size analysis of the pellets was carried out by sieves using an Erweka vibrating apparatus, with a set of eight standard sieves (100, 160, 250, 400, 630, 1000, 1600 μm). The sample size was 100.0 g and the shaking time was 5 minutes. The pellet size (geometric-weight mean diameter) and size distribution (geometric standard deviation) were estimated.

In case of optimized production *Rosin-Rammler-Sperling-Bennett* (RRSB) distribution function of particle size was also presented, based on the mass retained on the sieves, which is described by the following formula [21,73]:

$$R\% = 100 \cdot e^{-\left(\frac{x}{a}\right)^n} \qquad (14)$$

where

R% residual mass on the sieve

x particle size

a size at 36,8% of particles retained

n uniformity factor

Software for RRSB distribution was developed by our institute.

4.2.4.2. Drug release

Drug release from pellets containing *nystatin* was studied in 900 ml of pH 1.2 hydrochloric acid at 37±0.5°C, applying a paddle apparatus of Ph. Eur. 5. at 75 rpm (Erweka DT 700, Heusenstamm, Germany) examining 500 mg samples. Spectrophotometric determination was carried out according to previous examinations (λ = 306 nm, Jasco V-550 UV/VIS spectrophotometer, Japan). Mean and standard deviation (S.D.) was determined from three samples.

The dissolution kinetics of the preparation detected by both spectrophotometer and microbiological method, was determined by the *Weibull* distribution function, applied in the following form [1]:

$$m_t = m_\infty \left(1 - e^{-\left[\frac{(t-t_0}{\tau}\right]^\beta}\right) \quad (15)$$

where

m	dissolution (%) at time t
m_∞	dissolution (%) at infinite time
t_0	lag-time of dissolution
τ	mean dissolution time (theoretical time when 63.2% of the active agent is dissolved)
β	shape parameter of the dissolution profile

Our evaluation focused mainly on the effect of matrix forming agents on drug release kinetics. Shape parameter β and mean dissolution time τ were selected to characterize drug release and the correlation was determined between the values of the microbiological assay and the spectrophotometric measurement. Regarding these parameters, β_S and τ_S were determined from spectrophotometric data, β_M and τ_M were determined from microbiological assay.

4.2.4.3. Determination of biological activity by direct bioautography

One of the most widely applied methods among biological activity measurements is the direct bioautography. In this method microorganisms grown in a proper broth are spread on the surface of a TLC plate and then incubated. The surface of the TLC plate is covered with the broth to ensure the growth of microorganisms. Antimicrobial agents dripped on the plate develop inhibition zones which can be easily visualised by application of dehydrogenase activity detecting substances [56].

Biological activity of the samples was determined on silica gel plates applying 3-(4, 5-dimethyl-2-thiazolyl) -2, 5-diphenyl -2H- tetrazolium bromide – MTT (Sigma Aldrich, USA) to visualise antimicrobial activity. The applied test strain was *Candida albicans*, ATCC 90028. The TLC plates were: TLC DC - Alufolien Silica gel 60 F254 (Art. 1.05554, Merck, Darmstadt, Germany). Sample application on TLC plates was a series of 2-7 ng *nystatin* (Fig. 16.). Samples of microbiological detection and UV spectrophotometric determination were from the dissolution experiment. The diameter of inhibition spots was determined by the analysis of brightness distribution on TLC plate using 300 dpi scanned images and *ImageJ 1.45f* software (Wayne Rasband, National Institutes of Health, USA) for evaluation.

Figure 16. Inhibition spots on a sample TLC plate

4.2.4.4. Bioadhesivity test

The bioadhesivity of the prepared micropellets was investigated *ex vivo* by a wash-off test. A 1.5x1.5 cm piece of guinea pig ileum mucosa was fixed onto a plate at an angle of 45°. The examined section of ileum was previously rinsed in a Krebs buffer solution of the following composition:

- NaCl (119 mmol/L)
- KCl (4.7 mmol/L)
- $CaCl_2 \cdot 2H_2O$ (2.5 mmol/L)
- $NaHCO_3$ (20 mml/L)
- $MgCl_2 \cdot 7H_2O$ (1.17 mmol/L)
- KH_2PO_4 (1.18 mmol/L)
- EDTA (0.027 mmol/L)
- glucose (11 mmol/L)

Pellets (*n = ~50*) were gently spread onto the mucosa, then 50 ml of Krebs solution was applied to rinse at flow rate of 20ml/min. The number of pellets adhering to the tissue after rinsing were counted and compared to the total amount of the initial value in bioadhesion retention % [61].

4.2.4.5. Scanning electron microscopy examinations

Scanning electron microscope (JEOL, JSM 6300 Scanning Microscope, Japan) was used to study the surface and the shape of samples. For SEM evaluation the pellets were mounted on a worksheet and coated with fine gold. Acceleration voltage of 20.0 kV was used with 100x magnification.

4.2.4.6. Diffuse reflectance examinations

Diffuse reflectance measurement (*R%*) was carried out on solid samples applying an UV/VIS/NIR spectrophotometer (Jasco V-670, Japan) equipped with integrating sphere (diameter=60mm) and PbS detector between 1000-2000 nm in a 5 mm layered cell. Reflectance was evaluated according to the *Kubelka-Munk* formula [62]:

$$F(R\%) = \frac{K}{S} = \frac{(1-R\%)^2}{2R\%} \qquad (16)$$

where

R% intensity of diffusely reflected light

K absorption coefficient

S scattering coefficient

4.2.4.7. Swelling examinations

Swelling of pellets was determined using a calibrated stereomicroscope (Nikon SMZ 800 C-PS, Japan). During the examination n = ~ 50 pellets were suspended in 5 ml of distilled and degassed water. The increase in size of the pellets was monitored for 15 minutes and evaluated compared to the initial size [65].

4.2.4.8. Further dosage form examinations (bulk and tapped density, flowability, friability)

The bulk and tapped densities of the pellets were determined by standard methods. The tapped density was performed applying 1250 taps using a tapped density tester (J. Engelsmann, Ludwigshafen, Germany). The bulk and tapped density data were used to calculate the *Hausner's* [66] and *Carr's* [67] indices.

Flowability was examined using the apparatus described in the Ph. Eur. 7., 2.9.16. test, by application of a dry funnel calculating the angle of repose of 100.0 g sample preparation.

Friability examinations were carried out according to the Ph. Eur. 7. as well, using the apparatus in 2.9.7. test measuring 10.0 g of the sample. 100 rotations were made after the pellet's dust-control and then measured the loss of weight in % [68].

4.2.4.9. Stability test

Accelerated stability test of optimized product was carried out aiming the determination of the following parameters:

- k, degradation constant,
- $t_{½}$ half-life of the degradation and
- t_x expiration date.

Stability tests are based on the *Arrhenius* law:

$$k = A \cdot e^{-\frac{E_a}{RT}}, \tag{17}$$

At first order decomposition in case of *nystatin*, degradation half-life ($t_{1/2}$) can be calculated by the following way [74]:

$$t_{1/2} = \frac{0,693}{k} \tag{18}$$

The E_a activation energy can be determined by taking into account degradation constants at different test temperatures:

$$log\frac{k_2}{k_1} = \frac{E_a}{2,303R}\left(\frac{T_2 - T_1}{T_2 \cdot T_1}\right) \tag{19}$$

According to the *Arrhenius* equation results of long term stability tests can be predicted by calculating the degradation constants at different temperatures (in my experiment it was 40, 50 and 60°C), then representing the *log k-1/T* function, by extrapolation the decay at 25°C can be calculated [35,75].

In case of expiration date 5% decay of the API was allowed, applying the formula:

$$t_x = \frac{2,303}{k} log\frac{m_0}{m_0 - x} \tag{20}$$

Legends of the equations above:

k, k_1, k_2	degradation constants
A	pre-exponential factor (frequency factor)
E_a	activation energy

R	universal gas constant
T, T_1, T_2	absolute temperature
$t_{½}$	degradation half life
t_x	expiration date
m_0	initial API content
x	decayed API amount during t_x time

Simex Binder BF 115 thermostate was used to keep the samples on three different temperatures mentioned before at 75% relative humidity. Samples were taken monthly for 6 months. Total API content was determined by pulverizing the pellets and dissolving the API in 50 ml of methanol containing 5% acetic acid accelerating the dissolution by KL-2 Bühler shaking machine for 6 hours. After filtration *nystatin* content was determined (λ = 306 nm, Jasco V-550 UV/VIS spectrophotometer, Japan).

5. Results

5.1. Optimization results for high-shear pelletization

Considering the average particle size (y_1, $R = 0.981$), both process variables significantly influenced the particle agglomeration process through the model of the next formula:

$$y_1 = 1519.846 + 1.572x_1 - 266.98x_2 + 0.0558x_1x_2 - 0.0014x_1^2 + 9.829x_2^2 \quad (21)$$

The positive sign of the coefficients refers to an increasing effect while the negative sign indicates a decreasing effect on the corresponding response.

Increasing the binder flow rate the reduction of the average particle size was observed, which is probably due to the faster agglomeration, where more pellets were formed with smaller size within a shorter period. The impeller speed had opposite effect on particle size depending on its value. In the first stage (up to 750 rpm), the impeller helped the formation of larger particles, above 750 rpm, smaller particles were built due to intensive agitation which may hinder the further agglomeration of pellets (Fig. 17.).

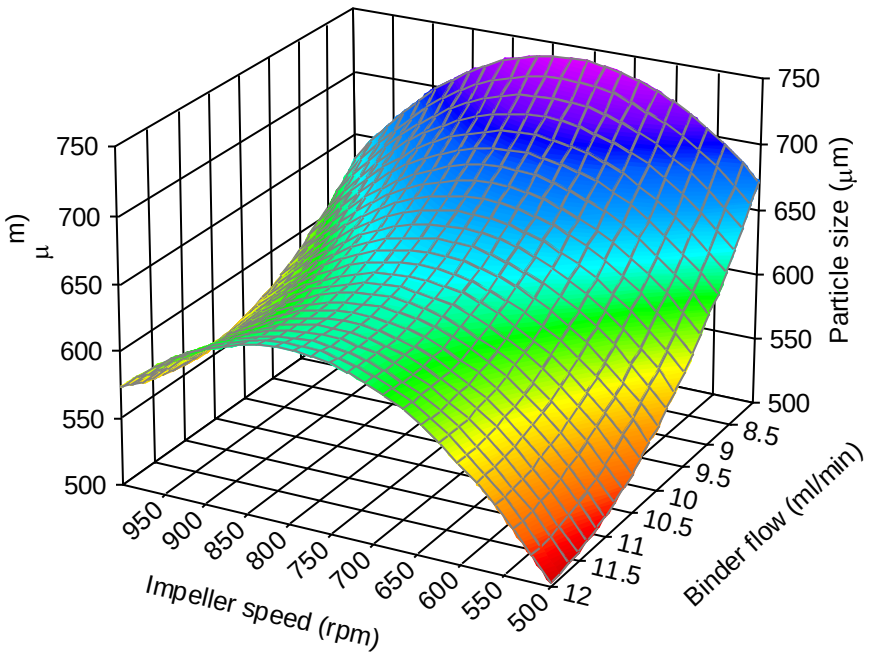

Figure 17. Effect of impeller speed and binder flow on the average particle size

Table VI. Measurements according to the experimental design

Trial	Controlled factor		
	x_1 **Impeller speed (rpm)**	x_2 **Binder flow (ml/min)**	y_1 **Particle diameter (μm)**
1	1000	12	583.8 ± 22.33
2	500	12	513.7 ± 26.67
3	1000	8	628.4 ± 33.42
4	500	8	669.8 ± 29.56
5	1000	10	596.4 ± 22.41
6	500	10	550.0 ± 15.67
7	750	12	628.4 ± 21.34
8	750	8	770.0 ± 39.12
9	750	10	632.7 ± 32.17

Table VII. Statistical evaluation of measurements

Response	Model *F*-value	Parameter	Coefficients					
			b_0	b_1	b_2	b_{11}	b_{22}	b_{12}
Particle diameter	15.20	Value	1519.846	1.572	− 266.979	− 0.0014	9.831	0.056
		Std error	464.235	0.463	84.792	2.65E− 04	4.141	0.023
		$p > \|t\|$	0.05	0.04	0.05	0.01	0.10 (NS)	0.10 (NS)

Diffuse reflectance spectra of pellet samples manufactured in the 9 experimental trials demonstrated significant differences depending on the impeller speed and binder flow rate (Fig. 18.). Pellet samples with large average particle diameter demonstrated an elevated spectral shift through $F(R)$ values, offering benefits for the in-process control, such as end-point determination of the pelletization process by NIRS. A linear regression was established between the particle size and transformed reflectance values according to the *Kubelka–Munk* formula (R=0.9842) (Fig. 19.).

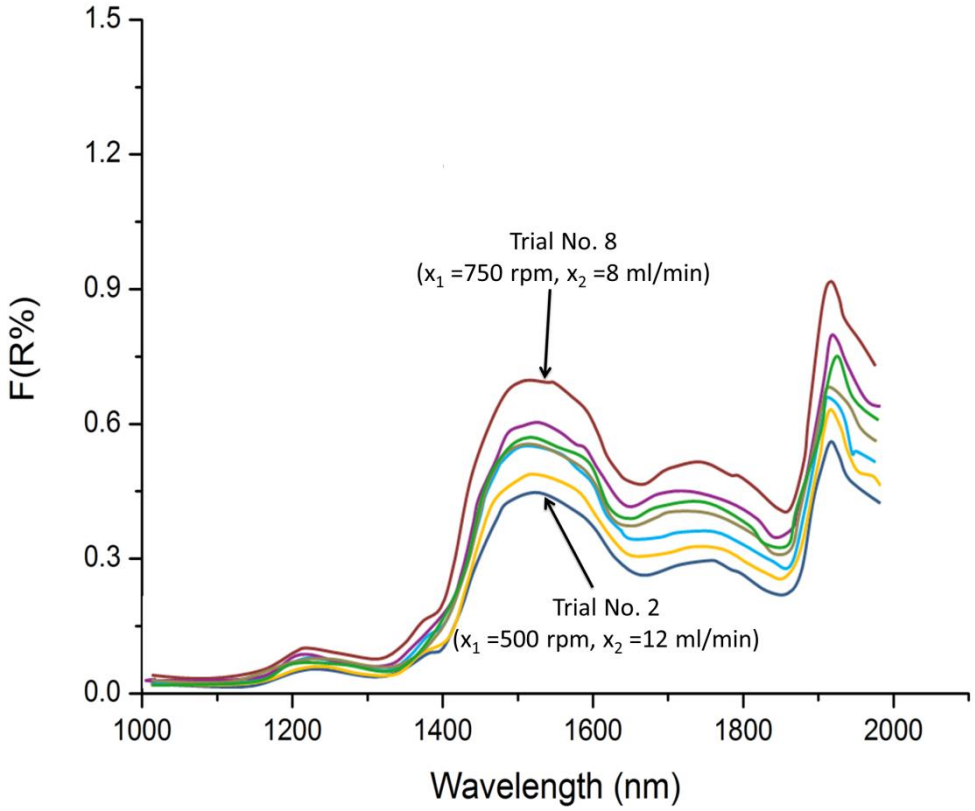

Figure 18. Diffuse reflectance spectra of samples according to *Kubelka-Munk* formula (see Chapter 4.2.4.6.)

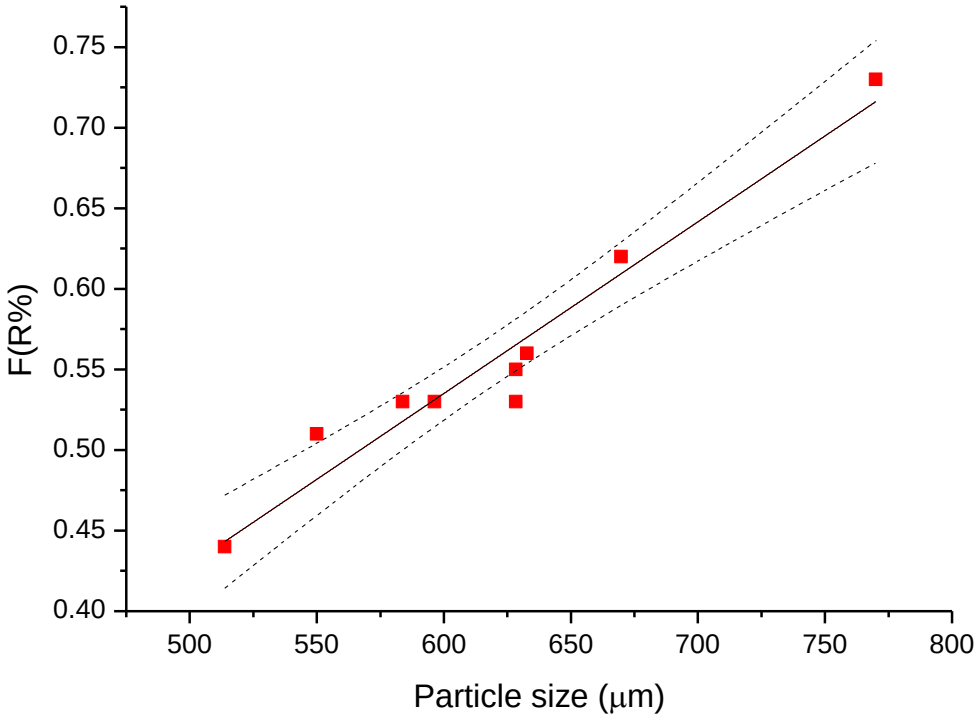

Figure 19. Correlation between the particle size of micropellets and diffuse reflectance spectra after *Kubelka-Munk* transformation at 1528 nm representing 95 % confidence interval

5.2. Results of examinations of nystatin micropellets

Results of our second manufacture based on preliminary examinations according the central composite experimental design (Table IV.) are described in Table VIII.

Table VIII. Matrix of the central composite experimental design (τ_S – mean dissolution time based on spectrophotometric data, τ_M – mean dissolution time based on microbiological assay, β_S – *Weibull's* shape parameter based on spectrophotometric data, β_M – *Weibull's* shape parameter based on microbiological assay)

Tr.	Examined factors			Response parameters (Mean±S.D., *n*=3)					
	x_1	x_2	x_3	Spectrophotometric data		Microbiological assay			
	Average particle size (µm)	CPL (%)	HEC (%)	τ_S (min)	β_S	τ_M (min)	β_M	Swelling (µm)	Bioadhesion retention (%)
1	700.0	4.27	0.73	119.5±10.8	0.3519±0.011	103.2±5.2	0.3462±0.0432	58.2±0.80	57.44±1.02
2	700.0	0.73	4.27	56.9±7.3	0.5362±0.012	49.0±2.1	0.5103±0.014	10.4±1.12	43.63±2.04
3	300.0	4.27	4.27	283.2±21.4	0.4023±0.042	278.0±13.6	0.3789±0.023	18.0±1.76	42.24±1.67
4	300.0	0.73	0.73	16.7±0.7	0.3134±0.010	11.3±1.1	0.2970±0.064	6.8±0.82	12.65±2.32
5	217.2	2.50	2.50	4.1±0.9	0.3898±0.047	3.6±0.4	0.3567±0.010	1.3±1.20	36.31±0.78
6	782.8	2.50	2.50	287.3±40.1	0.5131±0.028	227.3±2.4	0.5108±0.022	41.4±0.33	68.52±2.21
7	500.0	0.00	2.50	16.3±6.5	0.5044±0.035	11.9±1.2	0.4890±0.035	4.6±1.43	33.21±2.42
8	500.0	5.00	2.50	87.3±15.6	0.3918±0.057	71.8±8.6	0.3675±0.014	43.4±0.65	47.78±2.10
9	500.0	2.50	0.00	43.4±13.2	0.4251±0.030	42.4±10.9	0.4172±0.023	13.7±1.66	49.50±1.10
10	500.0	2.50	5.00	82.1±17.8	0.4978±0.038	51.8±7.4	0.4356±0.014	16.9±0.37	31.85±0.43
11	500.0	2.50	2.50	404.3±58.4	0.4112±0.013	316.8±21.4	0.3983±0.030	32.1±0.45	38.42±0.80
12	500.0	2.50	2.50	329.4±11.1	0.4212±0.027	320.7±24.2	0.4171±0.022	36.0±0.98	37.43±1.64
13	500.0	2.50	2.50	332.3±6.7	0.4154±0.057	249.1±31.1	0.4056±0.020	38.3±0.41	32.64±1.30
14	500.0	2.50	2.50	333.1±15.7	0.4190±0.021	313.4±18.6	0.3989±0.013	40.4±0.65	35.81±0.93
15	500.0	2.50	2.50	274.2±54.2	0.4287±0.049	269.5±13.3	0.3752±0.025	40.6±0.48	31.93±0.64

Our evaluation focused mainly on the effect of matrix forming agents on drug release kinetics and bioadhesion. Shape parameter β and mean dissolution time τ were selected to characterize drug release and the correlation was determined between the values of the microbiological assay and the spectrophotometric measurement. β_S and τ_S were determined from spectrophotometric data, β_M and τ_M were determined from microbiological assay.

Results of UV dissolution and microbiologically detected studies are summarized in Table VIII. The inhibition spot images of trial No. 4. evaluated by software *ImageJ 1.45f* are shown in Fig. 20.

Figure 20. Microbiologically Detected Dissolution (MDD) series of trial No. 4

Investigating the relationship between the spectrophotometric and microbiological detection, linear correlation can be observed both in mean dissolution time (R=0.9836) (Fig. 21.) and in the *Weibull's* shape parameter (R=0.9593) (Fig. 22.). However, performing a paired two-sample t-test, there is a significant difference between the means in both cases (p<0.05). This phenomenon is supposed to be due to the higher sensitivity of the microbiological assay. To confirm the sensitivity of the methods, the minimal limit of detection of *nystatin* was determined both using the microbiological and the spectrophotometric method. According to the linear range of calibration points the microbiological activity of *nystatin* was detected in concentration 0.8 ng/µl on TLC plate applying digital image analysis of inhibition spots, while limit of detection of spectrophotometric determination was 2 ng/µl. In both cases the applied solvent was pH 1.2 hydrochloric acid.

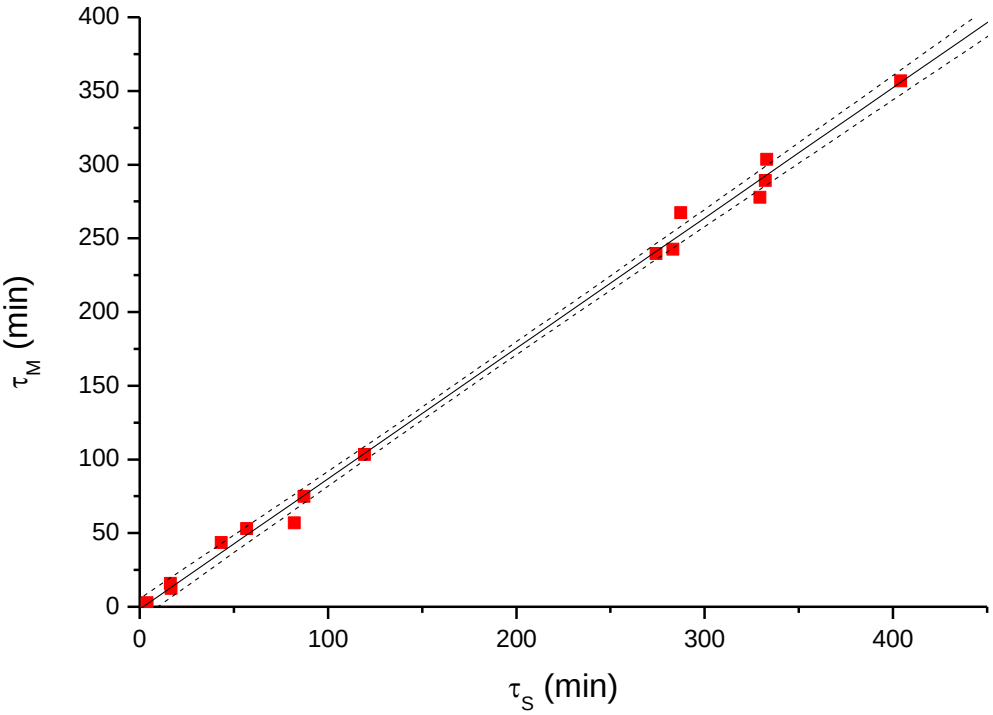

Figure 21. Correlation between the mean dissolution times calculated from the spectrophotometric and microbiological data (representing 95% upper and lower confidence intervals)

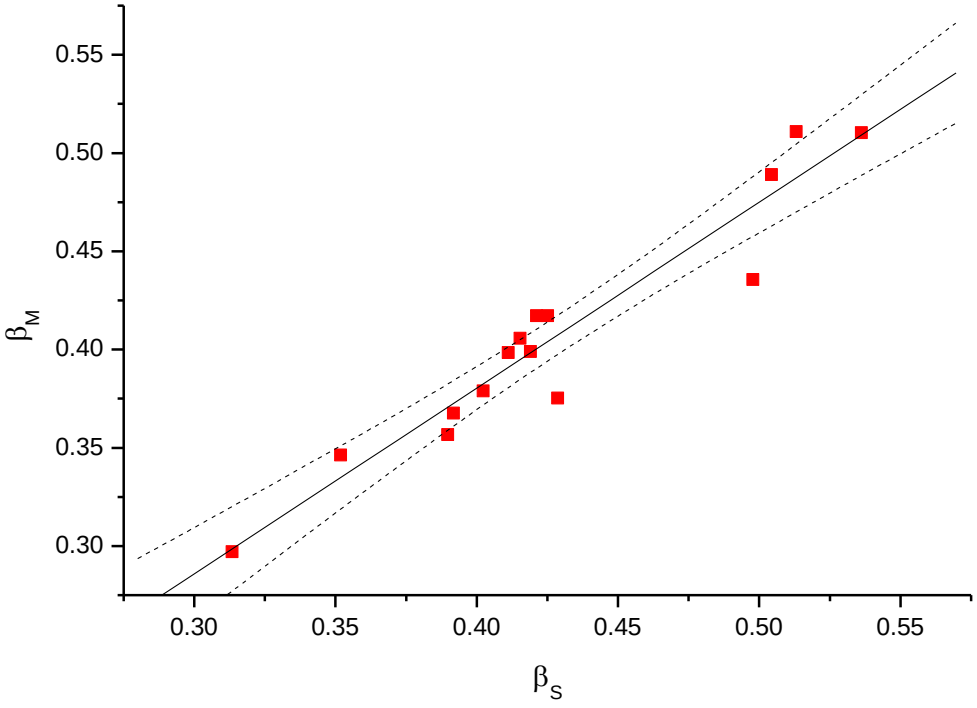

Figure 22. Correlation between the shape factors of the *Weibull* function calculated from spectrophotometric and microbiological data (representing 95% upper and lower confidence intervals)

Evaluating the dissolution curves, significant difference can be observed, since the presence of CPL and HEC slowed drug release remarkably, which is undesirable in this preparation. Fig. 23. presents the dissolution curves of trials 7, 9 and 12 as detected by both microbiological and spectrophotometrical method. The complete absence of CPL or HEC resulted in enhanced dissolution in trials no. 7 and 9.

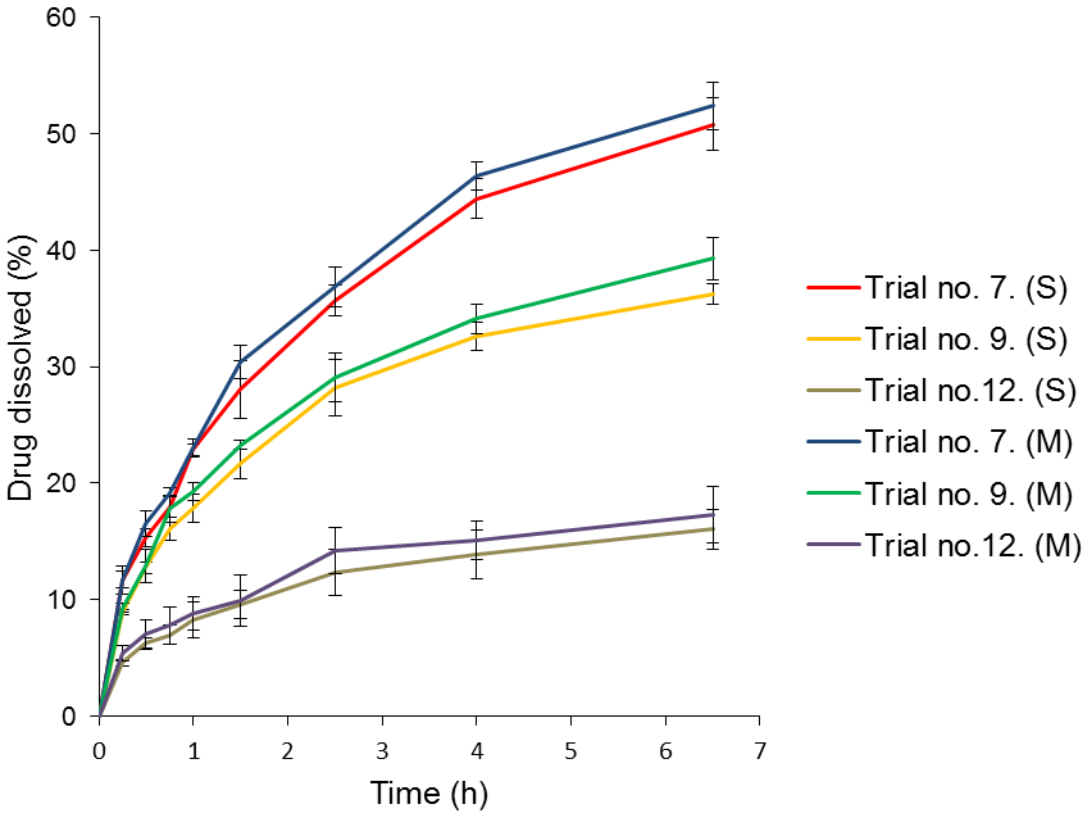

Figure 23. Dissolution of trials 7, 9. and 12 detected by both by spectrophotometric and microbiological method (S – spectrophotometric assay, M – microbiological assay)

Comparing and considering the measurements of the microbiological and spectrophotometric detection, the more sensitive microbiological tests were evaluated in further investigations. The equations of response surfaces represent the significant effects of factors x_1 and x_2 on the τ_M time parameter (R=0.9908), the β_M shape factor (R=0.8535), the bioadhesion retention time (R=0.8262) and the swelling (R=0.8415).

Table IX. represents the multiple regression statistical evaluation for significance and probabilities at 95% confidence interval of responses (*NS* = not significant).

Table IX. Statistical evaluation of the central composite factorial design

Response	Model *F*-value	Parameter	Coefficients										
			b_0	b_1	b_2	b_3	b_{12}	b_{13}	b_{23}	b_1^2	b_2^2	b_3^2	b_{123}
τ_M	21.32	Value	293.91	79.10	21.20	3.32	-49.79	-59.03	113.36	-89.24	-126.02	-123.41	-155.16
	(p=0.0048)	Std error	19.08	21.34	21.34	21.34	30.17	30.17	30.17	17.85	17.85	17.85	35.06
		p>|t|	-	0.0082	0.2619 (NS)	0.8480 (NS)	0.0961 (NS)	0.0620 (NS)	0.0078	0.0028	0.0008	0.0008	0.0044
β	9.84	Value	0.410	0.050	-0.032	0.034	-	-	-	-	-	-	-
	(p=0.0019)	Std error	9.16E-003	0.013	0.013	0.013	-	-	-	-	-	-	-
		p>|t|	-	0.0022	0.0279	0.0203	-	-	-	-	-	-	-
Swelling	8.89 (p=0.0028)	Value	26.81	12.56	14.23	-4.01	-	-	-	-	-	-	-
		Std error	2.74	3.76	3.76	3.76	-	-	-	-	-	-	-
		p>|t|	-	0.0065	0.0030	0.3087 (NS)	-	-	-	-	-	-	-
Bioadhesion	7.89 (p=0.0044)	Value	11.15	0.038	4.526	-0.649	-	-	-	-	-	-	-
		Std error	2.11	2.88	2.88	2.88	-	-	-	-	-	-	-
		p>|t|	-	0.0022	0.0181	0.6983 (NS)	-	-	-	-	-	-	-

According to the modified cubic response surface the average size of the pellets, its quadratic form, the quadratic form of CPL and HEC and the interaction between the CPL and the HEC influence the effect of *nystatin* significantly. Smaller size of the pellets results better dissolution due to the large specific surface. Pellets with average size from 500 to 1000 μm containing CPL and HEC in app, in ratio 1:1, have the slowest drug release profile (Fig. 24. and Fig. 25.). In this case the area of the maximum point is not recommended as aim during production.

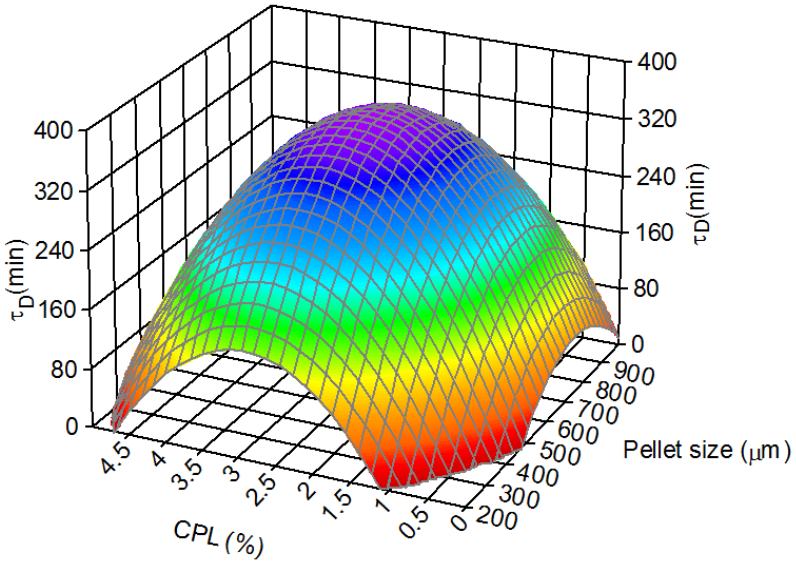

Figure 24. Effect of pellet size and CPL content on Mean Dissolution Time (2.5% HEC content)

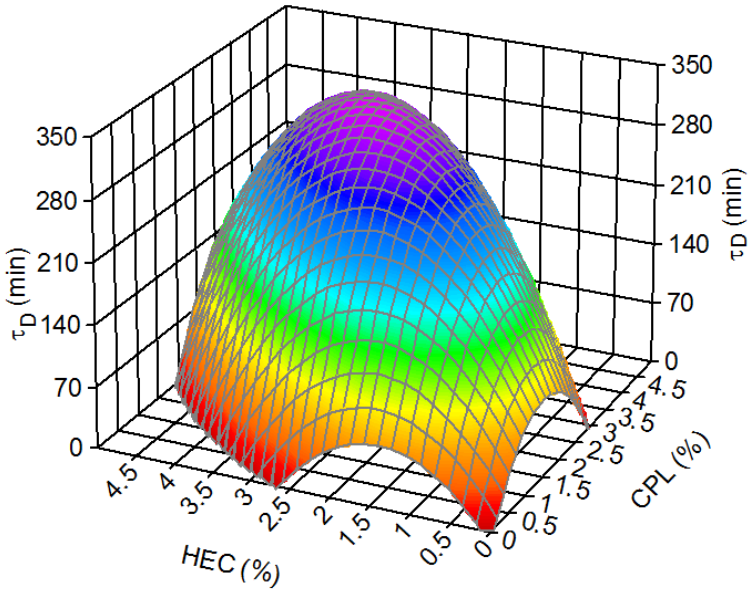

Figure 25. Effect of CPL and HEC content on Mean Dissolution Time (500 μm pellet size)

The *Weibull* function's shape parameter β is influenced significantly by pellet size, CPL and HEC content. The relationship is described with a linear model. The shape parameter increases with the increase of pellet size. Simultaneous increase of HEC and decrease of CPL results in a higher β value (Fig. 26. and Fig. 27.).

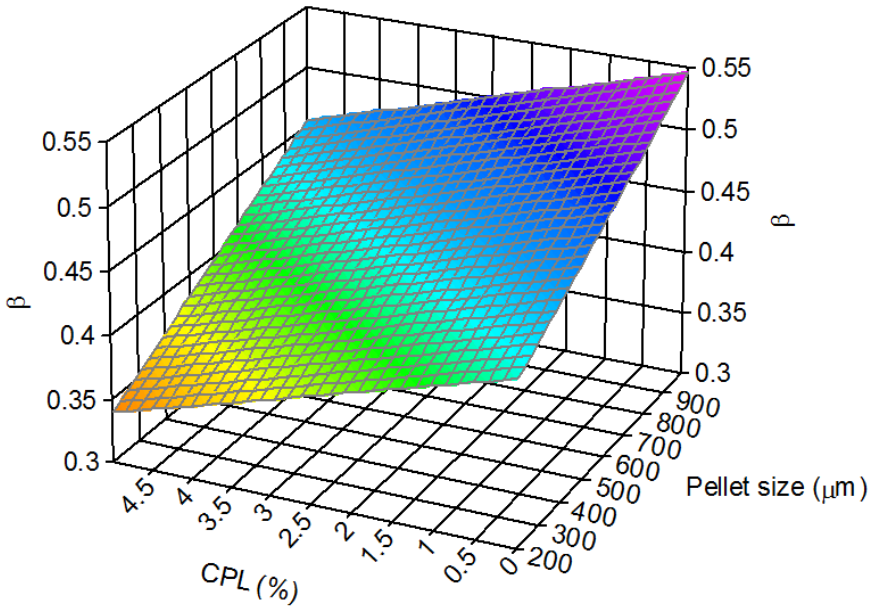

Figure 26. Effect of pellet size and CPL content on the *Weibull's* β_M shape parameter (2.5% HEC content)

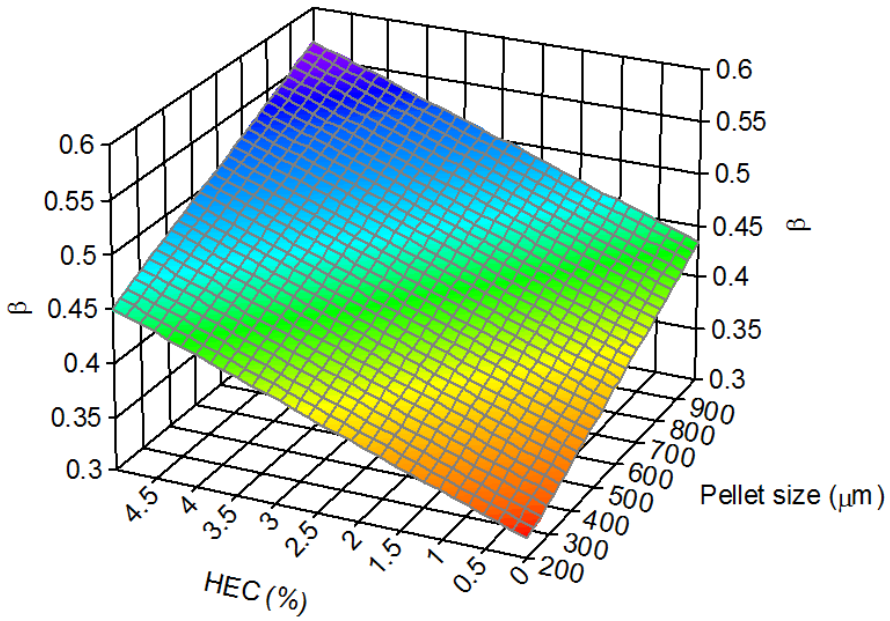

Figure 27. Effect of pellet size and HEC content on the *Weibull's* β_M shape parameter (2.5% CPL content)

Linear effect can be observed on Fig. 28. representing the swelling character of the samples. HEC has no significant effect, but increasing amount of CPL significantly increases the swelling ability.

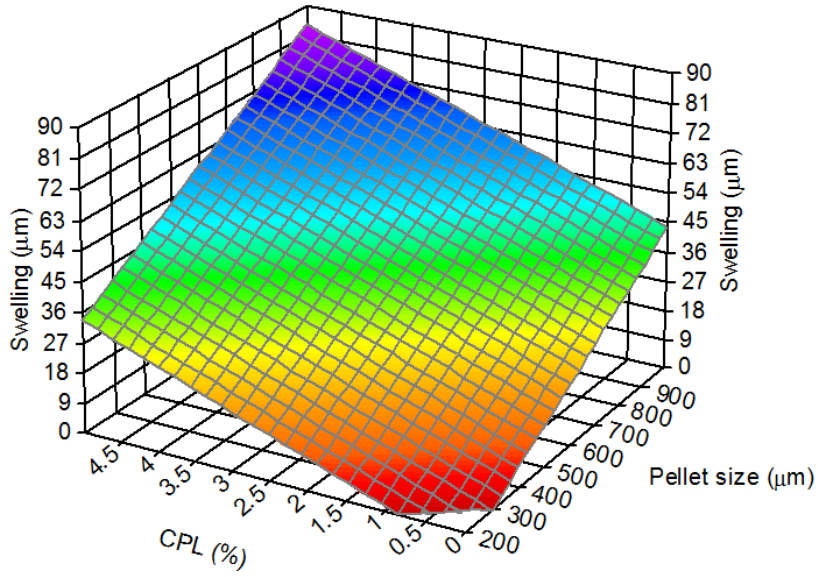

Figure 28. Effect of pellet size and CPL content on the swelling properties of pellets (2.5 % HEC content)

There are two significant factors (x_1 and x_2) concerning the linear model of bioadhesive retention. Contemporaneous increase in pellet size and CPL content produces higher bioadhesion rates (Fig. 29.). HEC content has no significant effect in this model.

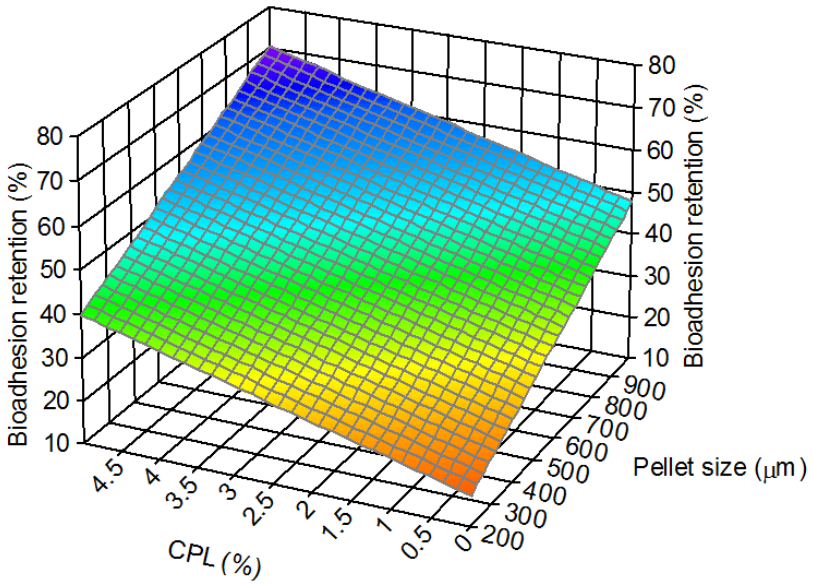

Figure 29. Effect of pellet size and CPL content on the ex vivo bioadhesion of pellets (2.5 % HEC content)

Trials 7, 9 and 12 were selected from the samples to be investigated by scanning electron microscopy with the same pellet size (500μm), but different ratios of CPL/HEC:

- Trial No. 7, CPL 0%, 5% HEC
- Trial No. 9, 5% CPL, 0% HEC
- Trial No. 12, 2.5% CPL, 2.5% HEC

The manufacturing process parameters were the same in all trials, thus the character of the surface of the pellets depends only on the CPL/HEC ratio. In trials No. 7, and 9 where either carbomer or hydroxyethylcellulose was used as bioadhesive agent, the surfaces of pellets were almost similarly porous. Samples from trial No. 12 containing CPL/HEC in ratio 1:1 were fine and glossy. This smooth surface is due to the congealment of the applied bioadhesive polymers which results slow release of the API (Fig. 30.).

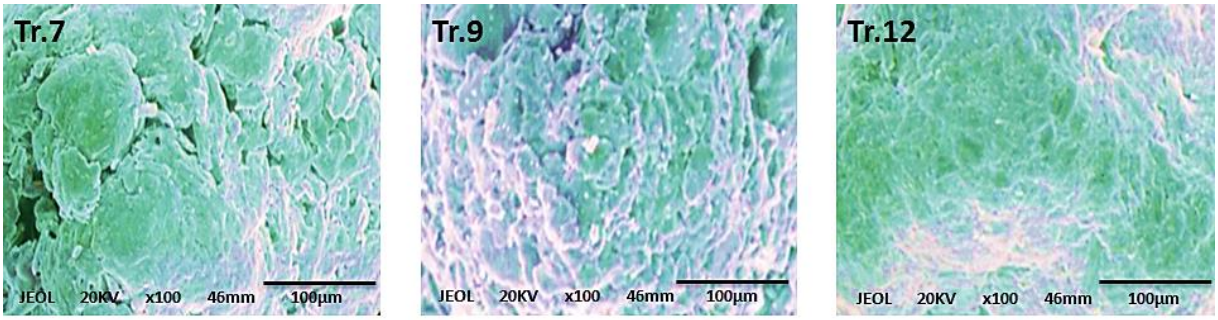

Figure 30. SEM image of micropellets from trials No. 7., 9., 12.

The diffuse reflectance spectra of pellet samples from trials No. 7, 9 and 12 with the same particle size of 500 μm were also analysed as a function of CPL and HEC content, which may refer to the surface characteristics of the samples [70]. Significant difference can be observed in trial No. 12, with elevated spectral shift caused by the glossy surface characteristics (Fig. 31.).

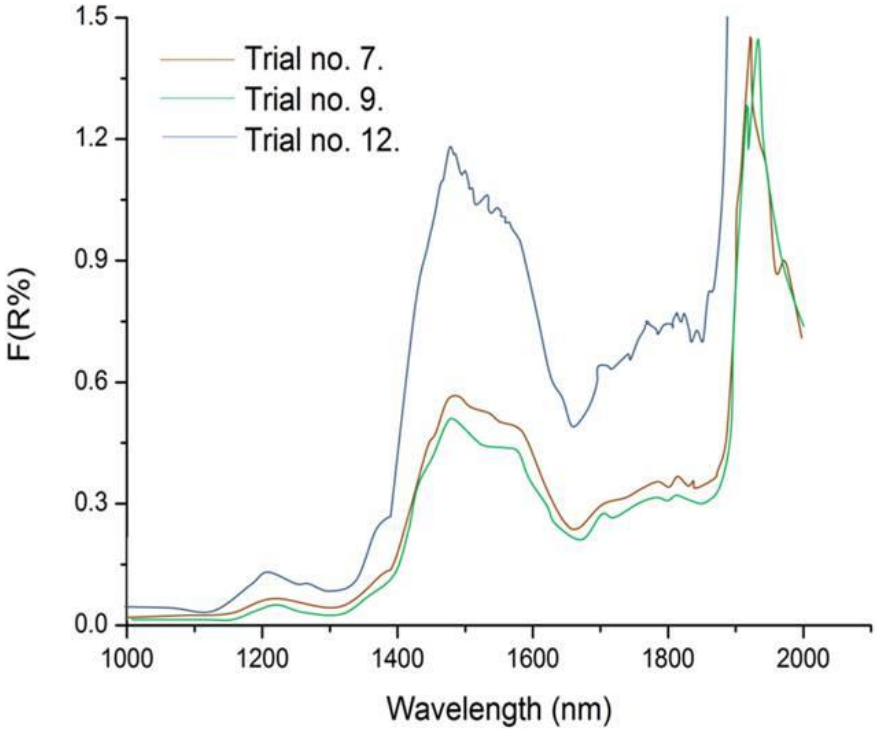

Figure 31. Diffuse reflectance spectra of pellet samples (Trials No. 7, 9 and 12) after *Kubelka-Munk* transformation (see Chapter 4.2.4.6.)

6. Discussion

The aim of the dissertation was to develop an optimized drug delivery system in order to treat gastrointestinal candidiasis. The fundamental point of an effective therapy may be a locally acting antifungal agent incorporated in a multiparticulate dosage form. As the active pharmaceutical ingredient, *nystatin* was chosen due to its advantageous properties of having contact antimicrobial effect with negligible absorption. As the dosage form micropellets were produced due to their good physical properties and large contact surface uniformly spreading through the GI tract. For production method among several possibilities high-shear pelletization was chosen, which is a reliable and quick method offering numerous facilities via adjustment of process parameters affecting the properties of the end-product. Optimized GIC therapy also requires long retention time on the surface of action which can be ensured by application of bioadhesive excipients, such as CPL and HEC. Summarizing the facts and observations, by production of *nystatin* based micropellets containing bioadhesive materials optimized GIC therapy can be reached.

In order to achieve the aims, preliminary examinations were carried out on a high-shear granulator to determine significant process parameters affecting the physical properties of micropellets focusing on the particle size distribution. These examinations were made according to a 3-level face-centred central composite experimental design examining the effect of impeller speed and binder flow rate on micropellet parameters.

After evaluation of the experiments a second order polynomial model was set up, which pointed to both factors as significant process parameters representing their effect as a saddle shape function. This experiment represented, that by applying extremities of the impeller speed (500 rpm and 1000 rpm) and liquid addition at speed of 10-12 ml/min together resulted relatively small particle size (500-550 μm). End-point of pelletization was determined by the measurement of the impeller torque. According to the experiments detection of NIR spectra after appropriate transformation could also serve important information of the process, since close (R=0.9842) correlation was observed between the particle size and the diffuse reflectance of the samples.

Results of these preliminary examinations were applied in the preparation of *nystatin* containing micropellets, adjusting process variables according to the previous experiences.

In the second production experimental design of full type with five centre points was set up. Examined factors were the following:

– average pellet size,
– CPL content and
– HEC content.

Investigated quality parameters of micropellets were:

– particle size distribution,
– flowability,
– hardness,
– surface characteristics,
– swelling,
– bioadhesion property and
– dissolution of nystatin determined by spectrophotometer and microbiological assay.

Evaluating the results important observation was the applicability of microbiologically detected dissolution based on direct bioautography, which had close correlation with the drug release determined by sphetrophotometric method regarding both the mean dissolution time (MDT) and the shape factor (β) of the *Weibull* distribution applied as a model for the dissolution studies. Extremities of the micropellet size (~200 μm and ~800 μm), CPL and HEC content (at both excipients 0 and 5%) short dissolution time could be achieved. According to the model established low value of shape factor, which was also the aim of the optimization, could be reached by reducing the pellet size and HEC content, but increasing CPL content. In case of swelling, particle size and CPL content was significant. Increasing CPL content and particle size swelling ratio also increased. Surface characteristics by SEM clearly represented the matrix formation of CPL and HEC when applied in the same amount, which was also confirmed by the diffuse reflectance spectra, since in this experiment it was not the indicator of the particle size, but the surface roughness of micropellets.

6.1. Optimization of GIC therapy

Gathering all experimental data and determining the optimization aims (short dissolution time and low β values with long retention time with appropriate swelling) software Design Expert v.7.0 (Stat-Ease Inc., Minneapolis, USA) was used to calculate the recommended parameters for the optimized GIC therapy by micropellet based drug delivery system.

Result of the optimization is production of *nystatin* containing micropellets with average size of 550μm, containing about 4.25% CPL and 0.75% HEC. To confirm the optimization result, a test sample was produced in triplicate.

Pellets production was carried out according to the previous experiences in a high-shear mixer (Pro-C-epT 4M8 Granulator, Belgium, Zelzate) with a three-blade impeller and a chopper. Powders were loaded into a 1000 ml bowl and premixed for 3 minutes. Ingredients and excipients were *5% nystatin* (Merck, Darmstadt, Germany), 45% α-lactose-monohydrate (DC, BDI, Zwolle, Netherlands), 45% microcrystalline cellulose (Avicel PH 105, FMC, Philadelphia, USA), 0.75% hydroxyethylcellulose (Hercules, Wilmington, USA) and 4.25% carbomer (Carbopol 934P, Hercules, Wilmington, USA). Quality of all materials used in the experiments was Ph. Eur. 7. The total dry mass was 100.0 g. 50 ml of purified water was used as granulation liquid at speed of 10 ml/min. Production was carried out at 25°C with 5 min net pelletization time applying 500 rpm impeller and 2000 rpm chopper speed.

Pelletization end-point (Fig. 32.) was determined according to the impeller torque in pelletization phase IV (see Chapter 3.3.6.2.2).

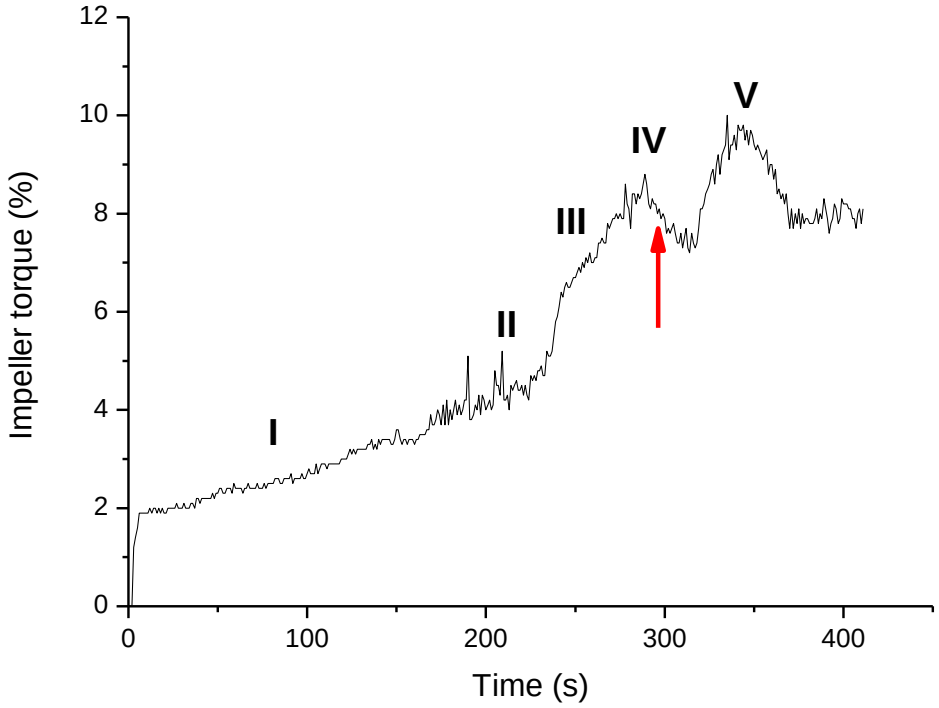

Figure 32. Pelletization end-point in case of optimized production (end-point marked with red arrow)

Examinations carried out were the following: average particle size, mean dissolution time, *Weibull* shape factor, flowability, Carr index, Hausner factor and friability.

Before examinations pellets were kept in a closed container for 24 h. Examination of these pellets were carried out in triplicate to test the optimization results (Table X.).

Table X. Results of examinations of optimized micropellets

Property	**Result**	**Desired value**
Average particle size	564.7±23.3 μm	550 μm
τ_D	5.7±2.1	5-10 min
β	0.3872±0.032	0.3-0.5
Bioadhesion retention	55.3±2.7 %	50-55%
Swelling	50.7±4.2 μm (8.8%±0.7%)	>5%
Flowability (angle of repose)	24.40°±3.18°	<25°
Carr index	10.71±0,23	<10
Hausner factor	1.12±0.05	<1.25
Friability	< 0.5%	<1%

Fig. 33. represents the RRSB particle size distribution function of the optimized micropellets with the following linearized relationship (R=0.9779):

$$y = -4.378 \cdot x + 11.169 \quad (22)$$

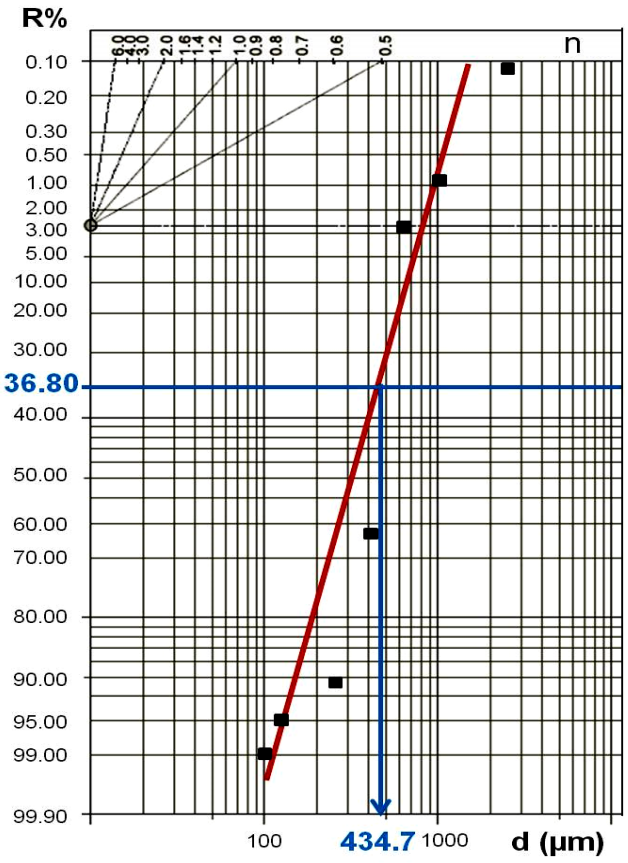

Figure 33. RRSB particle size distribution function of optimized micropellets

The particle size distribution of the optimized micropellets is monodiperse. According to the RRSB diagram the characteristic particle size parameter (*d*) at 36.8% is 434.7±15.3 µm and the uniformity factor: *n* = 4.378.

The dissolution curve of these samples is in Fig. 34. Results from stability tests are presented in Table XI. and Fig. 35.

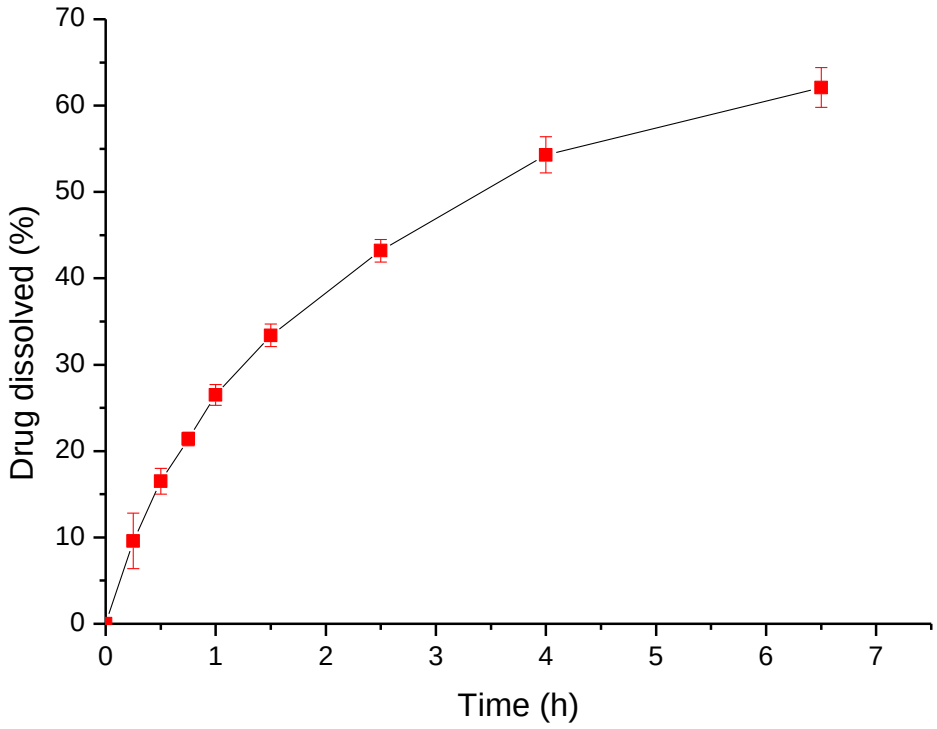

Figure 34. Dissolution curve of the optimized micropellets

Table XI. Results of stability tests

Temperature (°C)	*Nystatin* degradation	
	$t_{½}$ (months)	k ($month^{-1}$)
25	320.2	0.0022
40	76.4	0.0091
50	34.1	0.0203
60	2.3	0.3013

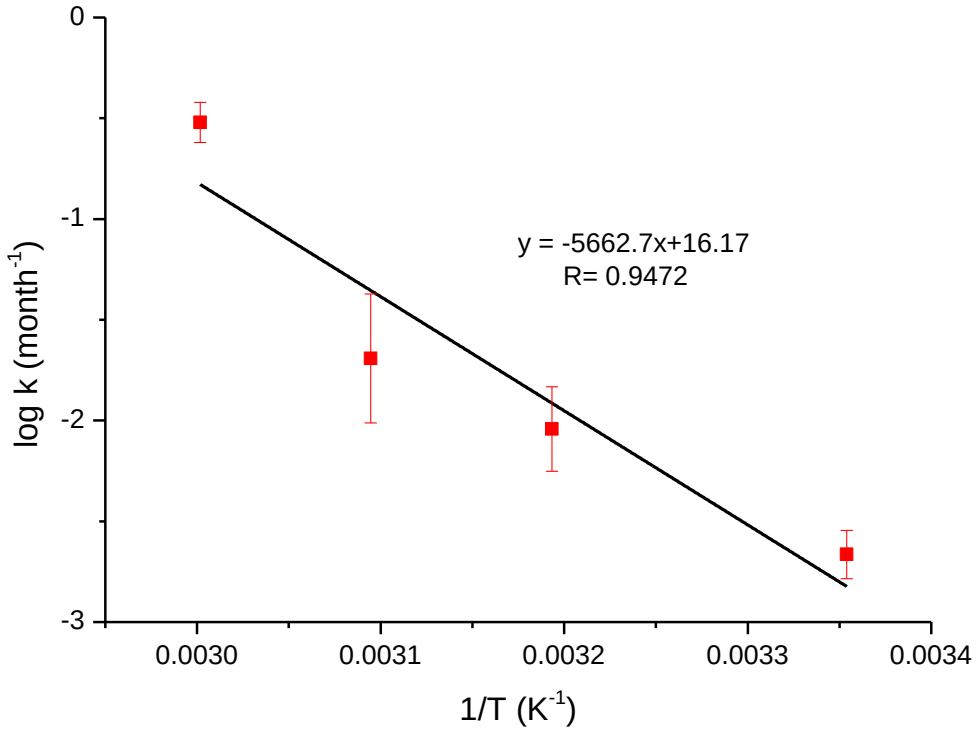

Figure 35. Stability test of the optimized sample

According to the Arrhenius law and my measurements, allowing 5% decay of the *nystatin*, expiration date: t_x = 34.18 months.

As it can be seen a thorough examination was carried out containing further tests according to the Ph. Eur. 7. beside the tests closely connected to the optimization results. According to the guidelines of Ph. Eur. 7. and scientific literature [67]] the test production fulfilled all the criteria specified before thus facilitating an optimized GIC therapy.

6.2. Summary of the new results

According to my preliminary and optimizational examinations new results of my research work are the following:

1. In my experiments impeller speed and binder flow rate were found as significant process parameters influencing the pellet size during high-shear pelletization.

2. It can be declared, that impeller torque and diffuse reflectance measurement can both be used in in-process control of high-shear pelletization including the determination of the end-point of the manufacturing process.
3. Measurement of diffuse reflectance was found to be an indicator of the surface characteristics of micropellets which was confirmed by SEM examinations.
4. According to the results application of Microbiologicaly Detected Dissolution (MDD) studies based on direct bioautography were able to modelize the antifungal effect of the *nystatin*.
5. Close correlation was found between spectrophotometric investigations and MDD studies.
6. Experiments verified that by incorporating bioadhesive materials, such as CPL and HEC in the pellet matrix, the residence time significantly increases on the surface of the mucous membranes.
7. According to the optimizational results of my research work optimal ratio of CPL:HEC was determined to be 17:3 to reach 50-55% bioadhesion retention and relatively quick dissolution (MDT=5-10min).
8. Optimal size of pellets in my experiments aiming GIC therapy is found to be 550μm.
9. Summarizing my results recommendation for the ingredients and their proportions in an optimized GIC therapy by production of micropellets with 550μm average particle size may be:
    - *nystatin* (5%)
    - *microcrystalline cellulose* (45%)
    - *α-lactose-monohydrate* (45%)
    - *carbomer* (4.25%)
    - *hydroxyethylcellulose* (0.75%)
10. Optimal process parameter recommendations in laboratory scale are:
    - 1000 ml glass pelletizing bowl
    - Initial temperature: 25°C
    - 100.0 g net weight of powders before liquid addition
    - 3 min premixing time
    - 5 min net pelletizing time
    - 1 min mixing after binder addition
    - 24 h drying of samples before examinations

- 500 rpm impeller speed
- 2000 rpm chopper speed
- 10ml/min binder flow rate (purified water)
- 50 ml total amount of binder liquid

7. Conclusion

During first experimental part the high-shear pelletization, the impeller speed and binder flow rate were observed as critical manufacturing parameters influencing the average particle size. Considering the formation of agglomerates, while the binder flow rate had a positive quadratic effect on the average particle size, the action of impeller was more complex depending on its rotation speed. The examined NIR diffuse reflectance spectra of pellet samples offer a fast instrumental method for in-process control and they can be due to the changed scattering which depended on the particle size of pellets. This experiment served as a base to adjust high-shear process variables according to therapeutical aims of my second experiment, focused on the gastrointestinal candidiasis therapy which is in accordance with the scientific literature.

The second part of my experimental work focused on the optimization of the *nystatin* based pharmaceutical therapy in GIC. Considering the parameters to be optimized, enhanced drug release and long contact time are the most important in terms of successful medication. The application of carbomer, a commonly used mucoadhesive excipient and hydroxyethylcellulose, a high stability and compatibility mucoadhesive agent in the optimized proportion in combination with optimized pellet size may be the key to a successful GIC therapy. According to the response surfaces obtained from the experimental design, the average pellet size of 550 μm, 85% carbopol: 15% hydroxyethylcellulose ratio (4.25% CPL and 0.75% HEC content) are approaching the optimal therapeutic effect, which result in approximately 50–55% bioadhesion retention, τ = 5–10 min drug release, β value of 0.32–0.37 and swelling index above 5%.

These estimations were confirmed in our test production where further investigations of the dosage form were carried out in order to prepare the applicant sample as a possibility for a more successful therapy in GIC.

List of Figures

List of Tables

References

[1] P. Costa, J. Manuel, S. Lobo: Modelling and comparison of dissolution profiles. Eur. J. Pharm. Sci. 13: 123–133.2001.

[2] F.O. Costa, J.J.S. Sousa, A.A.C.C. Pais, S.J. Formosinho: Comparison of dissolution profiles of Ibuprofen pellets. J. Control. Release 89: 199–212.2003.

[3] M. Siewert J. Dressman, C. Brown, V. Shah: FIP/AAPS guidelines for dissolution/in vitro release testing of novel/special dosage forms. Dissolution Technologies 6–15.2003.

[4] G. L. Amidon, H. Lennernas, V. P. Shah, J. R. Crison: A theoretical basis for a biopharmaceutic drug classification: the correlation of in vitro drug product dissolution and in vivo bioavailability. Pharmaceut. Res. 12: 413–420.1995.

[5] A. Dévay, I. Antal: A gyógyszeres terápia biofarmáciai alapjai. Medicina Könyvkiadó, Budapest, 2009.

[6] R. C. Schellekens, F. E. Stuurman, F. H. van der Weert, J. G. Kosterink, H. W. Frijlink: A novel dissolution method relevant to intestinal release behaviour and its application in the evaluation of modified release mesalazine products. Eur. J.Pharm. Sci. 30: 15–20.2007.

[7] J. J. Sousa, A. Sousa, F. Podczeck, J. M. Newton: Influence of process conditions on drug release from pellets. Int. J. Pharm. 144: 159–169.1996.

[8] R. E 2nd Cater: Chronic intestinal candidiasis as a possible etiological factor in the chronic fatigue syndrome. Med. Hypotheses 44:507–515.1995.

[9] A. Järvinen, S. Nykänen, L. Paasiniemi, T. Hirjärvi-Lahti, J. Mattila: Enteric coating reduces upper gastrointestinal adverse reactions to doxycycline. Clin. Drug Investig. 10: 323–7.1995.

[10] P. Macheras, A. Dokoumetzidis: On the heterogeneity of drug dissolution and release. Pharm. Res. 17: 108–12.2000.

[11] R. Chopra, G. Alderborn, F. Podczeck, J. M. Newton: The influence of pellet shape and surface properties on the drug release from uncoated and coated pellets. Int. J. Pharm. 239: 171–8.2002.

[12] R. Chatlapalli, B. D. Rohera: Physical characterization of HPMC and HEC and investigation of their use as pelletization aids. Int. J. Pharm. 161: 179–93.1998.

[13] I. Ghebre-Sellassie: Pharmaceutical Pelletization Technology: Drugs and pharmaceutical sciences. Marcel Dekker, New York, 1–13.1989.

[14] A. Faure, P. York, R. C. Rowe: Process control and scale-up of pharmaceutical wet granulation processes: a review. Eur. J. Pharm. Biopharm. 52: 269–77.2001.

[15] A. C. Jorgensen, P. Luukkonen, J. Rantanen, R. Schaefer, A. M. Juppo, J. Vliruusi: Comparison of torque measurements and near-infrared spectroscopy in characterization of a wet granulation process. J. Pharm. Sci. 93: 2232–43.2004.

[16] H. A. Rashid, J. Heinamaki, O. Antikainen, J. Yliruusi: Influence of the centrifugal granulating process on the properties of layered pellets, Eur. J. Pharm. Biopharm. 51: 227–234.2001.

[17] P. G. Paterakis, E. S. Korakianiti, P. P. Dallas, D. M. Rekkas: Evaluation and simultaneous optimization of some pellets characteristics using a 33 factorial design and the desirability function, Int. J. Pharm. 248: 51–60.2002.

[18] J.B. Schwartz, R. E. O'Connor: Optimization techniques in pharmaceutical formulation and processing. Editors: Banker GS, Rhodes CT. Modern Pharmaceutics. 3rd ed. Marcel Dekker, New York, 727–52.1997.

[19] D. Voinovich, M. Moneghini, B. Perissutti, E. Franceschinis: Melt pelletization in high shear mixer using a hydrophobic melt binder: influence of some apparatus and process variables. Eur. J. Pharm. Biopharm. 52: 305–13.2001.

[20] F. Zhou, C. Vervaet, J. P. Remon: Influence of processing ont he characteristics of matrix pellets based on microcrystalline waxes and starch derivatives, Int. J. Pharm. 147: 23–30.1997.

[21] A. Dévay: The Theory and Practice of Pharmaceutical Technology. University of Pécs, Pécs, 2013.

[22] P. Holm: Theory of granulation. Editor: Parikh D.M., Handbook of Pharmaceutical Granulation Technology, Marcel Dekker, New York, 7–23.1997.

[23] H. Rumpf: The strength of granules and agglomerates, In: Agglomeration, ed. K. W.A., Interscience, New York, 379–418.1962.

[24] D. M. Newitt, J.M. Conway-Jones: A contribution to the theory and practice of granulation, Trans. Instn. Chem. Engrs. 36: 422–442.1958.

[25] N. Ouchiyama, T. Tanaka: The propability of coalescence in granulation kinetics, Ind. Eng. Chem. Process Des. Dev. 14.3: 286–289.1975.

[26] H. G. Kristensen, P. Holm, T. Schæfer: Mechanical properties of moist agglomerates in relation to granulation mechanisms. Part I: Deformability of moist, densified agglomerates, Powder. Technol. 44: 227–237.1985.

[27] H. G. Kristensen, P. Holm, T. Schæfer: Mechanical properties of moist agglomerates in relation to granulation mechanisms. Part II: Effects of particle size distribution, Powder. Technol. 44: 239–247.1985.

[28] B. J. Ennis, J. Li, G. Tardos, R. Pfeffer: The influence of viscosity on the strength of an axially strained pendular liquid bridge, Chem. Eng. Sci. 45.10: 3071–3088.1990.

[29] B. J. Ennis, G. Tardos, R. Pfeffer: A microlevel-based characterization of granulation phenomena, Powder. Technol. 65: 257–272.1991.

[30] C. Vervaet, L. Baert, J. P. Remon: Extrusion-spheronisation. A literature review, Int. J. Pharm. 116: 131–146.1995.

[31] L. Briens, D. Daniher, A. Tallevi: Monitoring high-shear granulation using sound and vibration measurements, Int. J. Pharm. 331: 54–60.2006.

[32] D. Vojnovic, M. Moneghini, F. Rubessa: Optimalization of granulates in a high shear mixer by mixture design, Drug Dev. Ind. Pharm. 20.6: 1035–1047.1994.

[33] P. Holm: Effect of impeller and chopper design on granulating in a high speed mixer, Drug Dev. Ind. Pharm. 13.9-11: 1675–1701.1987.

[34] J. Kristensen, T. Schaefer, P. Kleinebudde: Direct pelletization in a rotary processor controlled by torque measurements. II: effects of changes in the content of microcrystalline cellulose. AAPS Pharmsci 2 .3: 24.2000.

[35] Encyclopedia of Pharmaceutical Technology, 3rd Edition, Editor: J. Swarbrick: Informa Healthcare USA Inc., New York, 2007.

[36] Handbook of Pharmaceutical Excipients, 5th Edition, Editor: R. C. Rowe, P. J. Sheskey, S. C. Owen: Pharmaceutical Press, London, 2006.

[37] S. R. Ghanta, R. Srinivas, C. T. Rhodes: Use of mixer torque measurements as an aid to optimizing wet granulation process. Drug Dev. Ind. Pharm. 10: 305–311.1984.

[38] R. C. Rowe: Mixer torque rheometry - further advances, Pharm. Tech. Eur. 8.8: 38–48.1996.

[39] S. Watano: Direct control of wet granulation processes by image processing system, Powder Technol. 117: 163–172.2001.

[40] J. Rantanen, S. Lehtola, P. Rämet, J. P. Mannermaa, J. Yliruusi: On-line monitoring of moisture content in an instrumented fluidized bed granulator with a multi-channel NIR moisture sensor, Powder Technol. 99: 163–170.2000.

[41] S. Ganguly, J. Z. Gao: Application of on-line Focused Beam Reflectance Measurement Technology in high shear wet granulation, The AAPS Journal 7(S2): Abstract No. T3216.2005.

[42] M. Whitaker, G. R. Baker, J. Westrup, P. A. Goulding, D. R. Rudd, R. M. Belchamber, M. P. Collins: Application of acoustic emission to the monitoring and end point determination of a high shear granulation process, Int. J. Pharm. 204: 79–91.2000.

[43] M. Knoke: Clinical pictures of orointestinal candidiasis. Fiction or reality? Mycoses 39 Suppl. 1: 40–43.1996.

[44] Martindale – The Complete Drug Reference, Editor: S. C. Sweetman: Pharmaceutical Press 36th Edition, London, 2009.

[45] J. D. Cleary, P. D. Rogers, S. W. Chapman: Variability in polyene content and cellular toxicity among deoxycholate amphotericin B formulations. Pharmacotherapy 23:572–578.2003.

[46] M. K. Kathiravan, A. B. Salake, A. S. Chothe, P. B. Dudhe, R. P. Watode, M. S. Mukta, S. Gadhwe: The biology and chemistry of antifungal agents: a review. Bioorgan. Med. Chem. 20: 5678–5698.2012.

[47] L. L. Patton, A. J. Bonito, D. A. Shugars: A systematic review of the effectiveness of antifungal drugs for the prevention and treatment of oropharyngeal candidiasis in HIV-positive patients. Oral Surg. Oral Med. Oral Pathol. Oral Radio. Endodont. 92: 170–179.2001.

[48] V. Grabovac, D. Guggi, A. Bernkop-Schnurch: Comparison of the mucoadhesive properties of various polymers. Adv. Drug Deliv. Rev. 57: 1713–1723.2005.

[49] J. M. Llabot, R. H. Manzo, D. A. Allemandi: Drug release from carbomer:carbomer sodium salt matrices with potential use as mucoadhesive drug delivery system. Int. J. Pharm. 276: 59–66.2004.

[50] J. S. Trier, D. J. Bjorkman: Esophageal, gastric, and intestinal candidiasis. Am. J. Med. 77: 39–43.1984.

[51] C. Maderuelo, A. Zarzuelo, J. M. Lanao: Critical factors in the release of drugs from sustained release hydrophilic matrices. J. Control. Release: Off. J. Control. Release Soc. 154: 2–19.2011.

[52] V. Ramana, S. Uppoor: Regulatory perspectives on in vitro (dissolution)/in vivo (bioavailability) correlations. J. Control. Release 72: 127–32.2001.

[53] R. F. Cosgrove, A. E. Beezer, R. J. Miles: A comparative study of the microbiological assays currently available for *nystatin* raw material. J. Pharm. Pharmacol. 31: 171–173.1979.

[54] O. V. Travkin, G. I. Lashkov, E. V. Komarov: Physiochemical characteristics of 3 states of the *nystatin* molecule. Antibiotiki 26: 519–522.1981.

[55] T. Higuchi, E. Brochmann-Hanssen, J. I. Bodin: Pharmaceutical Analysis. Interscience Publishers, New York, 1961.

[56] L. Botz, B. Kocsis, S. Nagy: Bioautography; in "Encyclopedia of Analytical Science, Ten-Volume Set"; Editor: P. Worsfold, A. Townshend, C. Poole. Elsevier Academic Press. 1: 271-277.2005.

[57] A. Dévay, B. Kocsis, Sz. Pál, A. Bodor, K. Mayer, S. Nagy: New method for microbiological detection of delivery process from dosage forms containing antibiotics. Eur. J. Pharm. Sci. 25: S81–S83.2005.

[58] R. Thies, P. Kleinebudde: Melt pelletization of a hygroscopic drug in a high shear mixer, Part I. Influence of process variables. Int. J. Pharm. 188: 131–43.1994.

[59] A. Dévay, K. Mayer, Sz. Pál, I. Antal: Investigation on drug dissolution and particle characteristics of pellets related to manufacturing process variables of high-shear granulation. J. Biochem. Biophys. Meth. 69: 197–205.2006.

[60] F. Langenbucher: Parametric representation of dissolution–rate curves by the RRSBW distribution. Pharm. Ind. 38: 472–7.1976.

[61] Z. Liu, W. Lu, L. Qian, X. Zhang, P. Zeng, J. Pan: In vitro and in vivo studies on mucoadhesive microspheres of amoxicillin. J. Control. Release: Off. J. Control. Release Soc. 102: 135–144.2005.

[62] I. Antal, R. Zelkó, N. Őrczey, J. Plachy, I. Rácz: Dissolution and diffuse reflectance characteristics of coated *theophylline* particles. Int. J. Pharm. 155: 83–9.1997.

[63] G. Reich: Near-infrared spectroscopy and imaging: basic principles and pharmaceutical applications. Adv. Drug Deliv. Rev. 57: 1109–43.2005.

[64] K. M. Morisseau, C. T. Rhodes: Pharmaceutical uses of near-infrared spectroscopy. Drug Dev. Ind. Pharm. 21: 1071–90.1995.

[65] P. Kleinebudde: Shrinking and swelling properties of pellets containing microcrystalline cellulose and low substituted hydroxpropylcellulose: I. Shrinking properties. Int. J. Pharm. 109: 209–219.1994.

[66] H. H. Hausner: Friction conditions in a mass of metal powder. Int. J. Powder. Metall. 3: 7–13.1967.

[67] R. L. Carr: Particle behaviour storage and flow. Br. Chem. Eng. 15: 1541–1549.1970.

[68] European Pharmacopoeia 7th Ed., Council of Europe, Strasbourg, 2013.

[69] Z. Muskó, J. Bajdik, K. Pintye-Hódi, P. Szabó-Révész, A. Kelemen, I. Erős: Preparation of pellets containing theophylline. Pharm. Ind. 64: 1194–8.2002.

[70] D. Murias, C. Reyes-Betanzo, M. Moreno, A. Torres, A. Itzmoyotl, R. Ambrosio, M. Soriano, J. Lucas, P.R.I. Cabarrocas: Black silicon formation using dry etching for solar cells applications. Mater. Sci. Eng. B – Adv. 177: 1509–1513.2012.

[71] P. Kleinebudde: The crystallite-gel-model for microcrystalline cellulose in wet-granulation, extrusion, and spheronization. Pharm. Res. 14.6: 804-809.1997.

[72] P. Holm, T. Schaefer, H. G. Kristensen: Granulation in high-speed mixers. Part VI. Effects of process conditions on power consumption and granule growth. Powder Technol. 43: 225–233.1985.

[73] T. Allen: Powder Sampling and Particle Size Determination. Elsevier, Amsterdam, 2003.

[74] J. M. T. Hamilton: The effect of pH and of temperature ont he stability and bioactivity of nystatin and amphotericin B. J. Pharm. Pharmac. 25: 401-407.1973

[75] A. Dévay, P. Kovács, I. Rácz: Optimization of chemical stability of diazepam in the liquid phase by means of factorial design. Int. J. Pharm., 6.3:5–9.1985.

[76] A. Dévay: Olvadék-diszeperziósls koacervációs eljárás gyógyszerek formulálása során. Doctoral candidate dissertation, Budapest, 1987.

[77] www.gea.com

Acknowledgements

I would like to thank to my PhD advisor

Dr. Attila Dévay

for his support and continuous help encouraging me during hard times of my research work, introducing me to the wonderful world of pharmaceutical technology and biopharmacy.

I would like to thank to my family and all my co-authors for their support in my work.

I thank all members of Institute of Pharmaceutical Technology and Biopharmacy for their help.